

Editor

Doç. Dr. Kemal BALIKÇI

gece
kitaplığı

**Research
and Evaluations
in the International
Field of Electrical
and Electronics
Engineering**

**October
2025**

Genel Yayın Yönetmeni / Editor in Chief • Eda Altunel

Kapak & İç Tasarım / Cover & Interior Design • Gece Kitaplığı

Birinci Basım / First Edition • © Ekim 2025

ISBN • 978-625-388-773-5

© copyright

Bu kitabın yayın hakkı Gece Kitaplığı'na aittir.

Kaynak gösterilmeden alıntı yapılamaz, izin almadan hiçbir yolla çoğaltılamaz. The right to publish this book belongs to Gece Kitaplığı. Citation can not be shown without the source, reproduced in any way without permission.

Gece Kitaplığı / Gece Kitaplığı

Türkiye Adres / Turkey Address: Kızılay Mah. Fevzi Çakmak 1. Sokak

Ümit Apt No: 22/A Çankaya/ANKARA

Telefon / Phone: 0312 384 80 40

web: www.gecekitapligi.com

e-mail: gecekitapligi@gmail.com

Baskı & Cilt / Printing & Volume

Sertifika / Certificate No: 42488

RESEARCH AND
EVALUATIONS IN
THE INTERNATIONAL
FIELD OF ELECTRICAL
AND ELECTRONICS
ENGINEERING

EDITOR

DOÇ. DR. KEMAL BALIKÇI

CONTENTS

Chapter 1

A Comprehensive Analysis of Power Quality Issues In Electric Power Systems

Serhat Berat EFE—1

Chapter 2

Artificial Intelligence-Based Approaches for Solar Panel Failure Detection

Seçil GENÇ, Rabia TEKEL DEMİR—17

Chapter 3

Investigation of Slot Parameters in Synchronous Motor Design via Finite Element Method and Machine Learning Approaches

İlyas ÖZER, Harun ÖZBAY,

Adem DALCALI—31

Chapter 4

Electrical Energy Consumption Forecasting Using Artificial Intelligence

Vekil SARI, Volkan GÖREKE—57

//

Chapter 1

A COMPREHENSIVE ANALYSIS OF POWER QUALITY ISSUES IN ELECTRIC POWER SYSTEMS

Serhat Berat EFE¹

¹ Assoc. Prof. Dr., Bandırma Onyedi Eylül University, Dept. Of Electrical Engineering, 10200, Bandırma. sefe@bandirma.edu.tr, ORCID: 0000-0001-6076-4166

INTRODUCTION

Power quality (PQ), as defined in IEEE Standard 1100, encompasses the appropriate powering and grounding of sensitive electrical equipment to ensure reliable and efficient operation. In contemporary electrical engineering, PQ remains a pivotal research domain, attracting sustained attention from engineers, scientists, and academic researchers due to its direct impact on system stability, equipment longevity, and energy efficiency. Diagnosing PQ disturbances demands a multidisciplinary expertise that spans electrical systems, signal processing, control strategies, and increasingly, artificial intelligence (AI). The complexity of PQ analysis is compounded by the interpretive ambiguity surrounding the term “research,” which often obscures the boundaries between theoretical exploration and practical implementation (Efe 2015).

PQ disturbances typically manifest as deviations in voltage or current waveforms, including voltage sags (commonly defined as a 10% reduction in nominal voltage), surges, momentary interruptions, harmonic distortions, and transient oscillations. These anomalies can lead to malfunction or premature failure of electrical equipment, underscoring the necessity for accurate identification of disturbance sources and the deployment of mitigation strategies (Cengiz 2024a). The diversity of PQ issues reflects the wide spectrum of variations in electrical power delivery across utility networks, often originating from customer-side operations such as improper grounding, transient switching events, nonlinear load behavior, and harmonic generation.

To address these challenges, the field has witnessed the emergence of advanced diagnostic and analytical tools, many of which leverage AI-driven methodologies. Intelligent algorithms, including machine learning and fuzzy logic systems, are increasingly employed to enhance fault detection, pattern recognition, and predictive maintenance capabilities. Notably, Electricité de France (EDF) has pioneered the use of signal processing techniques—such as wavelet transforms—for the detection and quantification of voltage sags and transient overvoltages, demonstrating the efficacy of time-frequency analysis in PQ evaluation (Akdeniz and Efe 2025; Isen 2022; Özer, Efe, and Özbay 2021).

Special attention is given to the role of intelligent systems in optimizing performance under dynamic load conditions and nonlinear operating environments. The integration of renewable energy sources (RES) introduces additional complexity, necessitating robust harmonic mitigation strategies to preserve grid stability and ensure compliance with international power quality standards. Although the scope of this review may

not encompass all emerging methodologies, it offers a valuable reference point for researchers and practitioners seeking to advance the field of power quality engineering. The findings underscore the importance of interdisciplinary approaches and the potential of intelligent technologies to drive sustainable and resilient electrical systems (Yuan et al. 2023).

The integration of renewable energy resources (RES), particularly wind and photovoltaic (PV) systems, introduces additional PQ complexities due to their intermittent and variable nature. Voltage and frequency fluctuations associated with RES integration pose significant challenges for grid stability and necessitate robust control mechanisms. As the global energy landscape shifts toward sustainable generation, the importance of maintaining high PQ standards becomes increasingly critical (EFE and KOCAMAN 2019).

Power quality (PQ) has emerged as a critical area of research in electrical engineering, particularly with the increasing complexity of modern power systems and the proliferation of nonlinear loads. Foundational studies, such as those by Bollen, have provided a structured classification of PQ disturbances—voltage sags, swells, transients, flicker, and harmonics—highlighting their detrimental effects on sensitive equipment and overall system reliability. These disturbances often originate from switching operations, load fluctuations, and grounding faults, necessitating robust diagnostic frameworks and mitigation strategies (Clement Veliz, Varricchio, and de Oliveira Costa 2022; Gong et al. 2021; Mishra 2019).

Among the various PQ issues, harmonic distortion remains one of the most persistent and technically challenging. The widespread adoption of power electronic devices has intensified harmonic generation, prompting extensive research into filtering techniques. Akagi's work on active power filters (APFs) demonstrated their effectiveness in dynamically suppressing harmonics under varying load conditions, outperforming traditional passive filters. Hybrid filtering approaches have since gained traction, offering improved compensation bandwidth and reduced energy losses. In parallel, signal processing techniques—particularly wavelet transforms—have proven valuable for analyzing PQ disturbances. Researchers such as Santoso applied discrete wavelet transforms (DWT) to detect and classify transient events, achieving superior time-frequency resolution compared to classical Fourier methods.

The integration of artificial intelligence (AI) into PQ analysis has further expanded the diagnostic and control capabilities of power systems. Intelligent algorithms, including fuzzy logic, neural networks, and support vector machines (SVMs), have been employed to model nonlinear

system behavior and automate disturbance classification (Shen et al. 2019; Shi et al. 2019; Wang and Chen 2019; Zhao, Shang, and Sun 2019). Dash and colleagues developed a fuzzy logic-based system capable of identifying multiple PQ events with high accuracy, even in noisy environments. More recently, machine learning techniques have been applied to large-scale PQ datasets, enabling predictive maintenance and real-time fault detection. These AI-driven approaches are instrumental in the development of smart grids and self-healing systems (Moradi et al. 2021; Ozkaya, Duman, and Isen 2025; Panoiu et al. 2023; Shahryari Nia, Sharifi, and Farzaneh 2022).

Renewable energy resources (RES), particularly wind and photovoltaic (PV) systems, introduce additional PQ challenges due to their intermittent and stochastic nature. Voltage and frequency fluctuations, as well as harmonic injection from inverter-based sources, complicate grid stability and require advanced control strategies. Blaabjerg's studies on grid-connected PV systems revealed significant harmonic propagation issues, prompting design modifications in inverter technology to mitigate adverse effects. AI-based forecasting models have also been developed to anticipate PQ disturbances based on weather patterns and load profiles, enhancing the resilience of renewable-integrated grids (Elkholy, El-Hameed, and El-Fergany 2018; Yasin, Ashida Salim, and Ab Aziz 2019).

Overall, the literature reflects a clear trend toward intelligent, adaptive, and integrated solutions for PQ management. While substantial progress has been made in harmonic mitigation and disturbance classification, ongoing challenges include standardizing AI methodologies and ensuring compatibility across diverse grid architectures. The dynamic behavior of RES continues to demand innovative approaches that balance sustainability with operational reliability. Ensuring high power quality and mitigating harmonic distortion are critical for the operational stability and efficiency of modern electrical systems.

This paper presents a comprehensive analysis of harmonic phenomena and power quality challenges across various electrical infrastructures, with particular emphasis on rotating electrical machines, intelligent control strategies, and renewable energy integration. The study synthesizes recent advancements in signal processing, fuzzy logic applications, and AI-based diagnostic techniques to address harmonic suppression and quality enhancement. By examining diverse technological approaches—including active and passive filtering, adaptive control algorithms, and smart grid-compatible architectures—the paper highlights the multidimensional nature of power quality improvement (Li et al. 2025; Tan and Ramachandaramurthy 2015).

1. METHODOLOGY

This study adopts a structured review-based methodology to synthesize and evaluate existing research on power quality (PQ) disturbances, harmonic mitigation strategies, and intelligent diagnostic techniques across various electrical systems. The approach is designed to provide a comprehensive understanding of the current technological landscape, identify prevailing challenges, and highlight emerging solutions relevant to both conventional and renewable energy-integrated networks (Rüstemli and Cengiz 2015).

Total Harmonic Distortion (THD) is a quantitative measure of harmonic distortion. Exceeding the limits defined by standards for THD can result in various adverse consequences. THD is calculated for voltage and current using Equations (1) and (2), respectively.

$$THD_V = \frac{1}{U_1} \sqrt{\left(\sum_{n=2}^{\infty} U_n^2 \right)} \quad (1)$$

$$THD_I = \frac{1}{I_1} \sqrt{\left(\sum_{n=2}^{\infty} I_n^2 \right)} \quad (2)$$

The IEC 61000-4-7 standard provides a comprehensive framework for the classification and measurement of harmonics, including detailed definitions for harmonic, interharmonic, and subharmonic components. These are mathematically represented by Equations (3) through (5), which facilitate spectral analysis of distorted waveforms in power systems.

$$\text{Harmonic: } f = kf_0 \quad (3)$$

$$\text{Interharmonic: } f \neq kf_0 \quad (4)$$

$$\text{Subharmonic: } f > 0 \text{ Hz and } f < f_0 \quad (5)$$

In these expressions k denotes a positive integer representing the harmonic order, f refers to the spectral component frequency of the signal, and f_0 indicates the fundamental frequency. Understanding and quantifying these components is essential for diagnosing and mitigating power quality issues. Harmonics, particularly those of higher orders, can

resonate with system impedances, leading to voltage amplification and potential equipment damage.

Interharmonics, which occur between integer multiples of the fundamental frequency, often arise from variable-speed drives and power electronic converters, contributing to flicker and instability. Subharmonics, with frequencies below the fundamental, can interfere with control systems and cause mechanical vibrations in rotating machinery (Efe 2016; Efe and Kocaman 2018; Efe, Özbay, and Özer 2019).

Harmonic distortion exerts a multifaceted impact on power system performance, manifesting in both operational inefficiencies and equipment vulnerabilities. Elevated harmonic currents increase the root mean square (RMS) values of electrical signals, resulting in excessive thermal stress across key components such as transformers, motors, illumination devices and capacitors (Cengiz 2024b; Isen and Duman 2024). This thermal overload not only accelerates insulation degradation but also shortens equipment lifespan. Moreover, harmonic-induced energy losses compromise overall system efficiency, leading to elevated operational costs and reduced power delivery quality. Protection systems are also susceptible; harmonics can interfere with the correct functioning of relays and circuit breakers, thereby undermining system reliability and safety.

Sample harmonic waveform is presented in Figure 1. In the Figure 1, there is a Total Harmonic Distortion (THD) value of 37.42%.

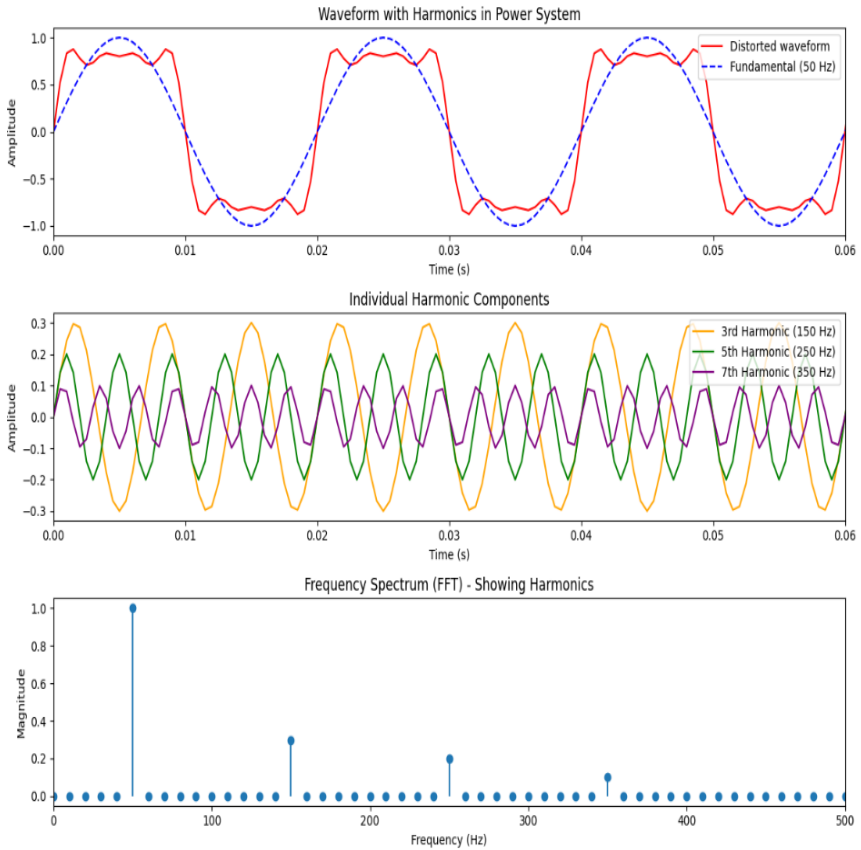


Figure 1. Sample harmonic waveform with frequency spectrum

In high-frequency ranges, harmonics may couple into adjacent communication lines, causing electromagnetic interference that disrupts data integrity and signal transmission. To mitigate these adverse effects and ensure compliance with established power quality standards—such as IEEE 519 and IEC 61000—utilities and facility managers implement a range of corrective strategies (Cengiz and Cengiz 2018). Passive filters, typically tuned LC circuits, are employed to absorb specific harmonic orders, while active power filters dynamically inject compensating currents to neutralize harmonic components in real time (Rüstemli and Sait Cengiz 2016). Transformer derating is also practiced to accommodate harmonic-induced heating, thereby preventing thermal overload (Rüstemli, Sait Cengiz, and Dinçer 2013).

Collectively, these measures serve to maintain Total Harmonic Distor-

tion (THD) within permissible thresholds, safeguarding both system stability and end-user equipment. A combined comparison table will make it very clear for readers to distinguish between system-level (IEEE 519) and equipment-level (IEC 61000-3-2 / 3-12) harmonic limits, which given in Table 1.

Table 1. *A combined comparison table between system-level (IEEE 519) and equipment-level (IEC 61000-3-2 / 3-12) harmonic limits*

Standard	Application Level	Harmonic Order (n)	Individual Limit	THD Limit (%)
IEEE 519-2014	Power System (PCC)	Any (n > 1)	<69 kV → 3%	<69 kV → 5%
			69–161 kV → 1.5%	69–161 kV → 2.5%
			>161 kV → 1%	>161 kV → 1.5%
IEC 61000-3-2	Equipment (<16A/phase)	3rd	2.30 A	–
		5th	1.14 A	–
		7th	0.77 A	–
		9th	0.40 A	–
		11th	0.33 A	–
		>39th	$0.15 \times (15/n)$ A	–
IEC 61000-3-12	Equipment (16–75A/phase)	5th	10%	8%
		7th	7%	8%
		11th	3.5%	8%
		13th	3%	8%

The methodology can be investigated and presented in four key stages.

1.1. Literature Selection and Classification

A systematic search was conducted across major scientific databases including IEEE Xplore, ScienceDirect, SpringerLink, and Scopus. Keywords such as power quality, harmonic distortion, active power filters, wavelet transform, fuzzy logic, AI in power systems, and renewable energy integration were used to identify relevant peer-reviewed articles, conference proceedings, and technical reports published between 2010 and 2025. Selected literature was categorized based on thematic relevance: (i)

harmonic analysis and filtering techniques, (ii) intelligent systems for PQ diagnosis, (iii) signal processing applications, and (iv) PQ challenges in renewable energy systems.

1.2. Analytical Framework

Each study was evaluated using a multi-criteria framework that considered the following dimensions: (a) type and severity of PQ disturbance addressed, (b) methodology or technology employed for mitigation or diagnosis, (c) system architecture and operational context, and (d) performance metrics such as total harmonic distortion (THD), voltage stability, and computational efficiency. Comparative analysis was performed to assess the effectiveness and scalability of different approaches under varying load and grid conditions.

1.3. Integration of Intelligent Techniques

Special emphasis was placed on the role of artificial intelligence (AI) and signal processing in enhancing PQ analysis. Studies employing fuzzy logic, neural networks, support vector machines (SVMs), and wavelet-based methods were examined in detail. The integration of these techniques was analyzed in terms of adaptability, real-time performance, and compatibility with smart grid infrastructures. Case studies involving AI-based monitoring systems and predictive maintenance tools were included to illustrate practical applications.

1.4. Renewable Energy Contextualization

Given the increasing penetration of renewable energy resources (RES), the methodology incorporated a focused review of PQ issues arising from wind and photovoltaic (PV) systems. Research addressing voltage and frequency fluctuations, inverter-induced harmonics, and grid synchronization challenges was prioritized. The analysis also considered hybrid control strategies and AI-enhanced forecasting models designed to stabilize PQ in RES-integrated environments.

This methodological framework ensures a balanced and rigorous examination of the literature, enabling the identification of technological trends, research gaps, and future directions in power quality engineering. The findings derived from this approach form the basis for the discussion and recommendations presented in subsequent sections.

2. DISCUSSION

Power disturbances in modern electrical systems have become increasingly critical due to the heightened sensitivity of power electronic components and control devices. Nonlinear loads, such as variable frequency drives and switched-mode power supplies, are primary sources of harmonic distortion, introducing non-sinusoidal currents into the network. Transient disturbances—often referred to as energy sinks—occur during abrupt switching events, such as capacitor bank energization, which injects high-frequency components into the system. Under fault conditions, energy is redirected from the network toward the fault path, and the direction of this energy flow can be accurately determined using waveform-recording instruments that sample three-phase voltage and current signals. In steady-state operation, the system is typically balanced, exhibiting constant instantaneous power. However, during non-steady-state conditions, the power flow becomes disturbed, and instantaneous power fluctuates throughout the network. Although the term “power quality” has gained formal recognition within the IEEE Standards Coordinating Committee (SCC), it remains less defined within the International Electrotechnical Commission (IEC), reflecting a gap in global standardization.

One of the most prevalent forms of power disturbance is voltage unbalancing, which is defined as a cyclic variation in voltage amplitude not exceeding 10%. Voltage unbalance arises when the root mean square (RMS) values of line voltages differ significantly across phases. This phenomenon is typically caused by asymmetrical line impedances, uneven distribution of single-phase loads, unbalanced three-phase loading, and the operation of controlled thyristor converters. Due to continuous switching of single and three-phase loads, perfect voltage balance is rarely achieved. In severe cases, voltage unbalance exceeding 5% can occur, particularly in single-phase circuits missing one or more phases. Such conditions can adversely affect three-phase motors, necessitating the use of phase monitors to prevent damage from single phasing. Voltage sags and swells—often triggered by load switching or fault events—are additional manifestations of PQ disturbances that compromise system reliability.

Harmonic distortion, current deviation, and frequency fluctuation represent another critical class of PQ issues, especially in systems integrating renewable energy sources (RES). The variability of RES output contributes to a diverse range of power anomalies, collectively referred to as Power Quality Disturbances (PQDs). Real-time monitoring of PQ parameters enables utilities to detect and respond to these issues promptly. Ideal current waveforms are characterized by constant frequency, magni-

tude, and a pure sinusoidal shape that remains in phase with the supply voltage. However, harmonics—defined as integer multiples of the fundamental frequency—distort these waveforms, leading to operational failures such as fuse blowing, breaker tripping, overheating of transformers and motors, and malfunctioning of protective relays. Among these, the third harmonic is particularly prominent and often blocked by grounding configurations in delta-wye transformers, which are designed to suppress zero-sequence components.

Rotating electrical machines are also significant contributors to harmonic distortion due to the non-sinusoidal nature of current flowing through stator windings. The resulting magneto-motive force (MMF) becomes distorted, leading to increased copper and iron losses. Copper losses, influenced by current distortion and skin effect phenomena, escalate under harmonic-rich conditions, while iron losses—also known as core losses—arise from magnetic field interactions within the machine core. These include eddy current losses and hysteresis losses, both of which degrade system efficiency and elevate core temperatures. Even minor voltage dips can have severe implications for system performance, particularly in distributed generation environments (Demir and Efe 2018; Efe 2018).

To address these challenges, advanced control strategies have been proposed for wind energy systems employing Doubly Fed Induction Generators (DFIGs). These generators offer dynamic control over rotor currents (i_{rd} and i_{rq}) and stator currents (i_{sd} and i_{sq}), enabling precise regulation of active and reactive power. In horizontal-axis wind turbines, DFIG-based configurations enhance grid compatibility and improve fault ride-through capabilities. Furthermore, active shunt power filters have been extensively studied for their effectiveness in improving grid energy quality. Comparative analyses of current control methods—ranging from hysteresis control to predictive and adaptive algorithms—demonstrate the potential of intelligent filtering techniques to mitigate PQ disturbances in both conventional and renewable-integrated systems (Senol et al. 2024). Application steps for harmonic analysis in power systems are summarized in Figure 2.

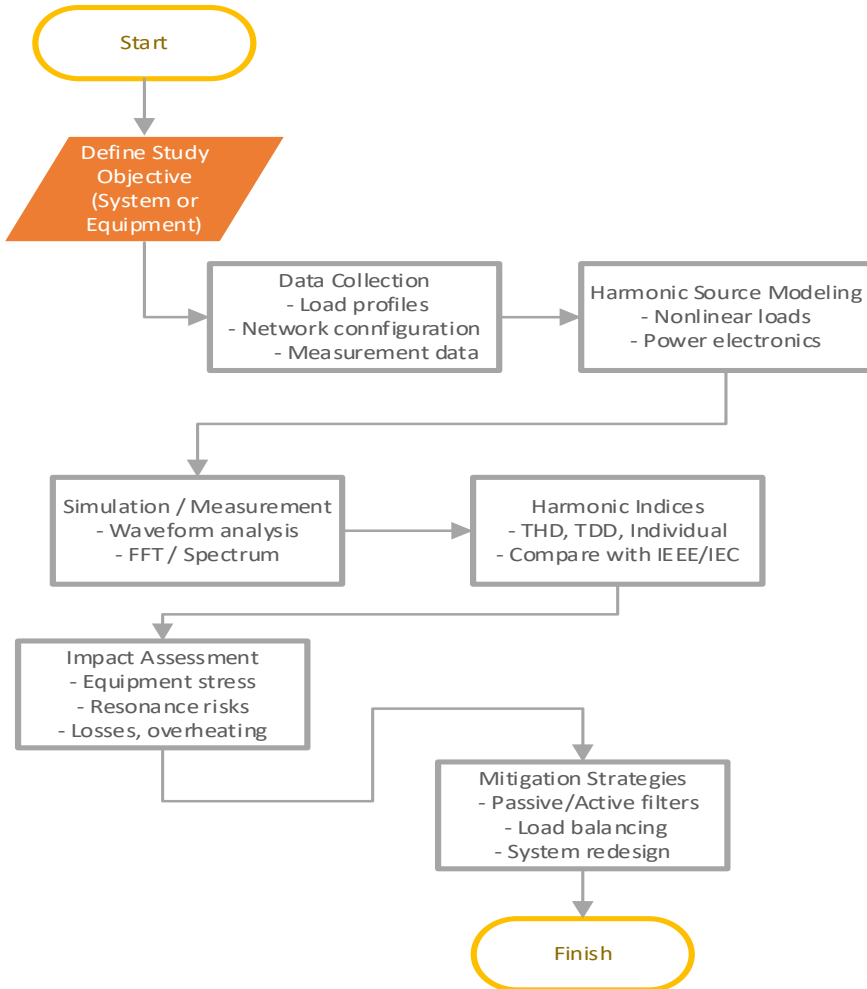


Figure 2. *Application steps for harmonic analysis*

3. CONCLUSION

This manuscript has presented a comprehensive exploration of power quality (PQ) disturbances, their underlying causes, and the evolving landscape of mitigation strategies within modern electrical systems. As power electronics and sensitive components become increasingly prevalent, the susceptibility to harmonic distortion, voltage unbalance, and transient anomalies has intensified, necessitating robust diagnostic and control frameworks. The review has highlighted the multifaceted nature of PQ issues, ranging from nonlinear load behavior and capacitor switching to the complex dynamics introduced by renewable energy sources (RES).

Advanced signal processing techniques, such as wavelet transforms, and intelligent systems—including fuzzy logic, neural networks, and machine learning algorithms—have demonstrated significant potential in enhancing real-time monitoring, fault classification, and adaptive control. These tools not only improve the precision of PQ analysis but also contribute to the development of resilient, self-regulating power networks. The integration of RES, while essential for sustainable energy transition, introduces additional PQ challenges that demand innovative solutions, particularly in inverter design, grid synchronization, and predictive forecasting (Feng, Mehmani, and Zhang 2020; Wang, Wang, and Liu 2017).

Furthermore, the discussion on rotating machines and their contribution to harmonic generation underscores the importance of addressing core and copper losses to maintain system efficiency. Control strategies for Doubly Fed Induction Generators (DFIGs) and active shunt filters exemplify the practical advancements aimed at stabilizing distributed generation systems.

In conclusion, the pursuit of high-power quality is inherently interdisciplinary, requiring collaboration across signal processing, control engineering, AI, and energy systems design. While the review may not be exhaustive, it offers a valuable synthesis of current methodologies and emerging trends, serving as a reference point for researchers and practitioners committed to advancing the reliability, efficiency, and sustainability of electrical power systems.

REFERENCES

- Akdeniz, Metin, and Serhat Berat Efe. 2025. "Forecasting of Harmonic Distortions in MV Distribution Network Caused by Illumination Devices." *Light and Engineering* 33(2):64–69. doi:10.33383/2024-088.
- Cengiz, Cigdem. 2024a. "Relationship of Braking Distance and Rear Headlight on Highways." *Light and Engineering* 32(2):29–36. doi:10.33383/2023-040.
- Cengiz, Cigdem. 2024b. "The Relationship Between Electricity Consumption from Outdoor Lighting and Economic Growth." *Light and Engineering* 32(4):14–21. doi:10.33383/2023-032.
- Cengiz, Mehmet Sait, and Çiğdem Cengiz. 2018. "Numerical Analysis of Tunnel LED Lighting Maintenance Factor." *IJUM Engineering Journal* 19(2):154–63. doi:10.31436/iijumej.v19i2.1007.
- Clement Veliz, Franklin, Sergio Luis Varricchio, and Cristiano de Oliveira Costa. 2022. "Determination of Harmonic Contributions Using Active Filter: Theoretical and Experimental Results." *International Journal of Electrical Power and Energy Systems* 137:1–11. doi:10.1016/j.ijepes.2021.107664.
- Demir, Dilan, and Serhat Berat Efe. 2018. "Analysis of PV Supplied SRM for Different Operating Conditions." Pp. 5–9 in *7th International Conference on Advanced Technologies (ICAT)*.
- Efe, Serhat Berat. 2015. "Harmonic Filter Application for an Industrial Installation." Pp. 31–34 in *2015 13th International Conference on Engineering of Modern Electric Systems, EMES 2015*.
- Efe, Serhat Berat. 2016. "Analysis of Power System Interharmonics." Pp. 1039–42 in *International Engineering, Science and Education Conference*.
- Efe, Serhat Berat. 2018. "Operational Analysis of a Switched Reluctance Motor Fed By PV System." Pp. 56–59 in *International Conference on Electrical and Electronics Engineering*.
- Efe, Serhat Berat, and Behçet Kocaman. 2018. "Harmonic Analysis of a Small-Scale Wind Turbine." Pp. 1–4 in *7th ICAT 2018*.
- EFE, Serhat Berat, and Behçet KOCAMAN. 2019. "Harmonic Analysis of a Wind Energy Conversion System with Small-Scale Wind Turbine." *International Journal of Energy Applications and Technologies* 5(4):168–73. doi:10.31593/ijeat.441563.
- Efe, Serhat Berat, Harun Özbay, and İlyas Özer. 2019. "Dynamic Voltage Restorer Application to Eliminate Power System Harmonics." Pp. 705–9 in *International Engineering and Natural Sciences Conference (IENSC 2019)*.
- Elkholy, Mahmoud M., M. A. El-Hameed, and A. A. El-Fergany. 2018. "Harmonic Analysis of Hybrid Renewable Microgrids Comprising Optimal Design of Passive Filters and Uncertainties." *Electric Power Systems Research* 163:491–501. doi:10.1016/j.epr.2018.07.023.
- Feng, Cong, Ali Mehmani, and Jie Zhang. 2020. "Deep Learning-Based Real-Time

- Building Occupancy Detection Using AMI Data.” *IEEE Transactions on Smart Grid* 11(5):4490–4501. doi:10.1109/TSG.2020.2982351.
- Gong, Jie, Dayi Li, Tingkang Wang, Wenhao Pan, and Xinzhi Ding. 2021. “A Comprehensive Review of Improving Power Quality Using Active Power Filters.” *Electric Power Systems Research* 199:1–15. doi:10.1016/j.epsr.2021.107389.
- Isen, Evren. 2022. “Determination of Different Types of Controller Parameters Using Metaheuristic Optimization Algorithms for Buck Converter Systems.” *IEEE Access* 10:127984–95. doi:10.1109/ACCESS.2022.3227347.
- Isen, Evren, and Serhat Duman. 2024. “Optimization of the Different Controller Parameters via OBL Approaches Based Artificial Ecosystem Optimization Involving Fitness Distance Balance Guiding Mechanism for Efficient Motor Speed Regulation of DC Motor.” *Soft Computing* 28(17–18):9455–81. doi:10.1007/s00500-024-09693-0.
- Li, Fei, Yongxin Zhang, Qiang Feng, Yang Liu, Xing Zhang, and Mingyao Ma. 2025. “Comprehensive Design of Active Damper for Suppression of Harmonic Resonance in Renewable Energy System.” *Electric Power Systems Research* 245:1–9. doi:10.1016/j.epsr.2025.111564.
- Mishra, Manohar. 2019. “Power Quality Disturbance Detection and Classification Using Signal Processing and Soft Computing Techniques: A Comprehensive Review.” *International Transactions on Electrical Energy Systems* 29(8):1–42. doi:10.1002/2050-7038.12008.
- Moradi, Arash, Jalil Yaghoobi, Abdulrahman Alduraibi, Firuz Zare, Dinesh Kumar, and Rahul Sharma. 2021. “Modelling and Prediction of Current Harmonics Generated by Power Converters in Distribution Networks.” *IET Generation, Transmission and Distribution* 15(15):2191–2202. doi:10.1049/gtd2.12166.
- Özer, İlyas, Serhat Berat Efe, and Harun Özbay. 2021. “CNN / Bi-LSTM-Based Deep Learning Algorithm for Classification of Power Quality Disturbances by Using Spectrogram Images.” *International Transactions on Electrical Energy Systems* 31(12):1–16. doi:10.1002/2050-7038.13204.
- Ozkaya, Burcin, Serhat Duman, and Evren Isen. 2025. “Enhanced Manta Ray Foraging Optimization Algorithm Involving Fuzzy-Based Fitness-Distance Balance Method for Estimation of Unidentified Parameters of PEMFC Model.” *Electrical Engineering* 107(6):7203–61. doi:10.1007/s00202-024-02935-2.
- Panoiu, Manuela, Caius Panoiu, Sergiu Mezinescu, Gabriel Militaru, and Ioan Baci. 2023. “Machine Learning Techniques Applied to the Harmonic Analysis of Railway Power Supply.” *Mathematics* 11(6):1381. doi:10.3390/math11061381.
- Rüstemli, Sabir, and Mehmet Sait Cengiz. 2015. “Active Filter Solutions in Energy Systems.” *Turkish Journal of Electrical Engineering & Computer Sciences* 23:1587–1607. doi:10.3906/elk-1402-212.
- Rüstemli, Sabir, M. Sait Cengiz, and Furkan Dinçer. 2013. *Elektrik Tesislerinde Harmoniklerin Aktif Filtre Kullanılarak Yok Edilmesi ve Simülasyonu*.

Vol. 2.

- Rüstemli, Sabir, and Mehmet Sait Cengiz. 2016. "Passive Filter Solutions and Simulation Performance in Industrial Plants." *Bitlis Eren Univ J Sci & Technol* 6(1):39–43.
- Senol, Murat, I. Safak Bayram, David Campos-Gaona, Kristian Sevdari, Oliver Gehrke, Benjamin Pepper, and Stuart Galloway. 2024. "Measurement-Based Harmonic Analysis of Electric Vehicle Smart Charging." in *2024 IEEE Transportation Electrification Conference and Expo, ITEC 2024*. Institute of Electrical and Electronics Engineers Inc.
- Shahryari Nia, Kourosh, Mohammad Ali Sharifi, and Saeed Farzaneh. 2022. "Tidal Level Prediction Using Combined Methods of Harmonic Analysis and Deep Neural Networks in Southern Coastline of Iran." *Marine Geodesy* 45(6):645–69. doi:10.1080/01490419.2022.2116615.
- Shen, Yue, Muhammad Abubakar, Hui Liu, and Fida Hussain. 2019. "Power Quality Disturbance Monitoring and Classification Based on Improved PCA and Convolution Neural Network for Wind-Grid Distribution Systems." *Energies* 12:1–26. doi:10.3390/en12071280.
- Shi, Xiaoying, Hui Yang, Zhibang Xu, Xiujun Zhang, and Mohammad Reza Farahani. 2019. "An Independent Component Analysis Classification for Complex Power Quality Disturbances with Sparse Auto Encoder Features." *IEEE Access* 7:20961–66. doi:10.1109/ACCESS.2019.2898211.
- Tan, Rodney H. G., and Vigna K. Ramachandaramurthy. 2015. "A Comprehensive Modeling and Simulation of Power Quality Disturbances Using MATLAB/SIMULINK." in *Power Quality Issues in Distributed Generation*. InTech.
- Wang, Huihui, Ping Wang, and Tao Liu. 2017. "Power Quality Disturbance Classification Using the S-Transform and Probabilistic Neural Network." *Energies* 10:1–19. doi:10.3390/en10010107.
- Wang, Shouxiang, and Haiwen Chen. 2019. "A Novel Deep Learning Method for the Classification of Power Quality Disturbances Using Deep Convolutional Neural Network." *Applied Energy* 235(September 2018):1126–40. doi:10.1016/j.apenergy.2018.09.160.
- Yasin, Zuhaila Mat, Nur Ashida Salim, and Nur Fadilah Ab Aziz. 2019. "Harmonic Distortion Prediction Model of a Grid -Connected Photovoltaic Using Grey Wolf Optimizer - Least Square Support Vector Machine." Pp. 1–6 in *2019 9th International Conference on Power and Energy Systems, ICPEES 2019*. Institute of Electrical and Electronics Engineers Inc.
- Yuan, Wenqian, Xiang Yuan, Longwei Xu, Chao Zhang, and Xinsheng Ma. 2023. "Harmonic Loss Analysis of Low-Voltage Distribution Network Integrated with Distributed Photovoltaic." *Sustainability (Switzerland)* 15(5). doi:10.3390/su15054334.
- Zhao, Wenjing, Liqun Shang, and Jinfan Sun. 2019. "Power Quality Disturbance Classification Based on Time-Frequency Domain Multi-Feature and Decision Tree." *Protection and Control of Modern Power Systems* 4(1):1–6. doi:10.1186/s41601-019-0139-z.

//

Chapter 2

ARTIFICIAL INTELLIGENCE-BASED APPROACHES FOR SOLAR PANEL FAILURE DETECTION

Seçil GENÇ¹, Rabia TEKEL DEMİR²

1 Ondokuz Mayıs Üniversitesi, Elektrik-Elektronik Mühendisliği Bölümü, Atakum/
SAMSUN

email: secil.yilmaz@omu.edu.tr

ORCID ID: <https://orcid.org/0000-0002-3754-0209>

2 Yesilirmak Electricity Distribution Company, Atakum/SAMSUN

email: rabia.tekel@yedas.com

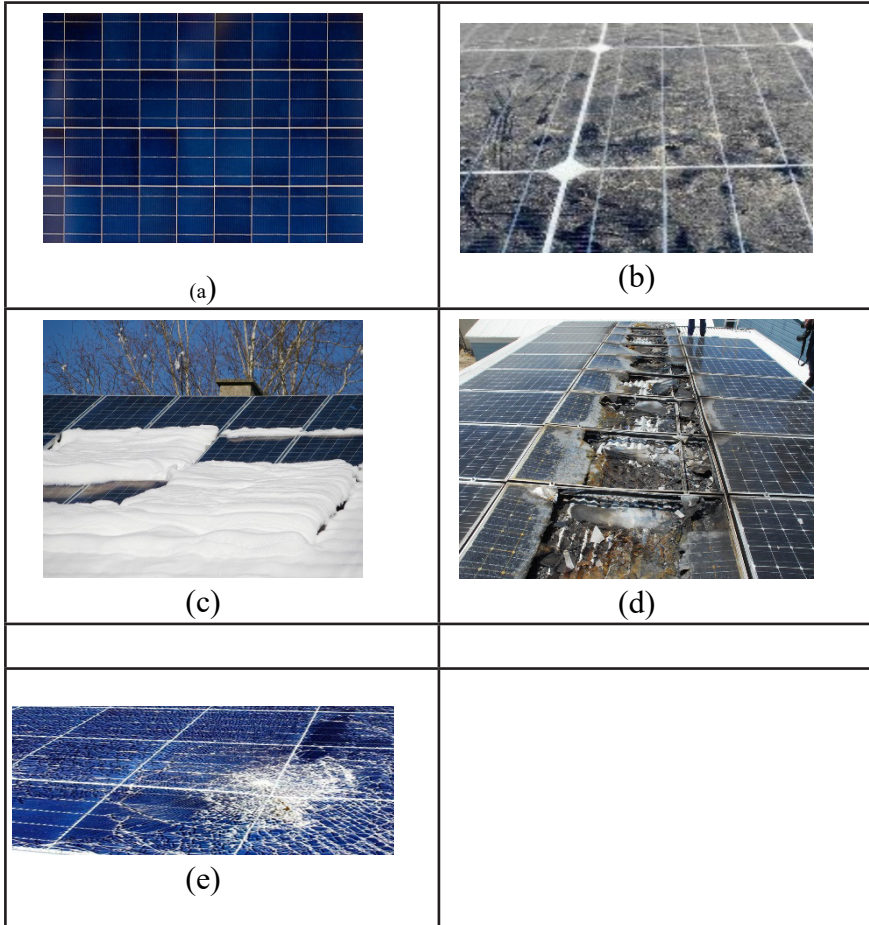
ORCID ID: <https://orcid.org/0009-0006-2179-7719>

1. SOLAR PANEL FAILURE DETECTION

Photovoltaic (PV) systems are very sensitive to outside conditions, which can strongly influence how well they work. Renewable energy has many advantages compared to fossil fuels because it is sustainable and more friendly to the environment. Among all renewable sources, solar energy is especially important since it is clean, long-lasting, and has low operating costs. Among the most popular and efficient methods of harnessing solar energy are photovoltaic (PV) systems. These systems convert sunlight directly into electricity, offering a clean and efficient way to produce power both in large power plants and in smaller, distributed systems.

The long-term success of PV systems depends a lot on finding problems early, fixing them on time, and keeping good maintenance practices. Over time, PV systems can lose efficiency because of different reasons. These include physical problems (like cracks or broken panels), environmental effects (such as shading, dust, bird droppings, or snow), electrical issues (like hot spots, loose connections, or inverter faults) (Jalal, Khalil, & ul Haq, 2024), and even production defects. Many of these faults can be seen visually—for example as dark spots, cracks, hazy areas, discoloration, or corrosion. These signs can help in detecting faults and monitoring the system. If such problems are not found in time, they reduce efficiency and can even cause long-term damage, leading to big financial losses. That is why monitoring and fault detection in PV systems are not only technical tasks but also very important from both economic and environmental points of view.

In recent years, artificial intelligence (AI) has become a very useful tool for this purpose. Monitoring can be done more quickly, accurately, and efficiently with AI techniques than with conventional maintenance methods.



PV panel images classified as (a) clean, (b) soiled, (c) snow-covered, (d) electrically damaged, and (e) physically damaged (Kaggle, 2025)

2. DESCRIPTION OF THE PROCESS

Fig. 2 presents the flowchart of the fault detection approach. Images of solar panels are gathered and pre-processed in the first step to improve their quality and highlight any potential flaws. Histogram equalization, contrast adjustment, edge sharpening, noise reduction, and resizing are examples of pre-processing techniques. These techniques ensure consistency in the input data and bring out significant details in the images.

After preparing the images, they are used for both training and testing with traditional machine learning and deep learning methods. Traditional algorithms like support vector machines (SVM), k-nearest neighbors (k-NN), decision trees, and random forests depend on manually designed features such as texture, edges, and statistical properties. In contrast, deep

learning models learn important features directly from the raw images, eliminating the need for hand-crafted feature extraction.

Convolutional neural networks (CNNs) serve as the main framework. Several well-known CNN architectures are tested, including Inception-Net (captures multi-scale features with parallel convolutions), AlexNet (introduces deeper layers and ReLU activation), VGGNet (applies uniform 3×3 filters), ResNet (uses residual connections to avoid vanishing gradients), DenseNet (strengthens feature reuse with dense links), and LeNet (a simple but effective early CNN). To handle limited datasets, transfer learning with pre-trained models is applied, which helps improve accuracy and speed up training. Model performance is evaluated using standard metrics such as accuracy, precision, recall, and F1-score. In addition, cross-validation and confusion matrix analysis are carried out to assess generalization ability and performance on specific fault types. The findings indicate that CNN-based deep learning methods achieve higher accuracy in detecting complex faults like micro-cracks, delamination, hotspots, and surface contamination. In contrast, traditional machine learning algorithms can still perform adequately when the fault patterns are relatively simple (Alatwi et al., 2024).

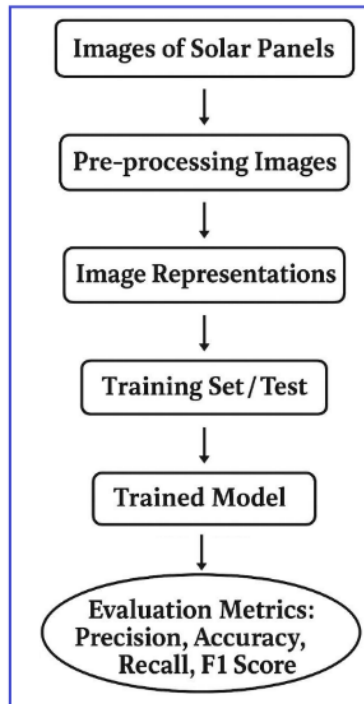


Fig 1. Flowchart of the fault diagnosis method.

A) Pre-Processing of Solar Images

This flowchart explains the steps of applying a machine learning model to solar panel images. First, the raw images are gathered and pre-processed to improve their quality and reduce distortions. Next, the images go through segmentation, and useful features are extracted to provide the model with clear information. One portion of the dataset is used for testing, and the other for training. After learning from the training data, we evaluate the model's performance on fresh data. We examine various metrics, such as accuracy, precision, recall, and F1 score, to assess the model's performance (Pathak & Patil, 2023).

B) Pre-Trained CNN Models

Models that have already been trained like ResNet, AlexNet, Inception, LeNet, VGGEfficientNet, DarkNet, ShuffleNet, DetNet, SqueezeNet, and YOLO are commonly used in deep learning for image classification tasks. These CNN architectures, when applied through transfer learning, have greatly contributed to the progress of artificial intelligence. The following describes some of the most widely used CNN models in the context of solar panel fault detection.

AlexNet Architecture

The AlexNet architecture includes several convolutional layers with filter sizes of 11×11 , 5×5 , and 3×3 , followed by max-pooling layers, as shown in Fig. 2. Compared to more traditional functions like sigmoid or tanh, one of its primary innovations is the use of the ReLU activation function after each convolutional and fully connected layer, which aids in speeding up training. To reduce overfitting, dropout is applied in the fully connected layers, and data augmentation is used to increase the size of the training set. The model is trained with stochastic gradient descent and momentum to improve convergence. Additionally, AlexNet uses GPU acceleration, which allows training very large datasets in a reasonable time (Swapna et al., 2020) .

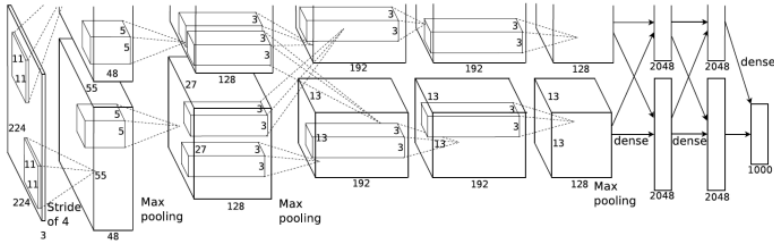


Fig 1. AlexNet Architecture (Krizhevsky et al., 2012)

LeNet-5 Architecture

The architecture has seven main layers (not counting the input layer), which include convolutional, pooling (subsampling), and fully connected layers, as shown in Fig. 3. It works by applying a series of convolution operations, each followed by a pooling step—originally average pooling, though later versions often used max pooling. After that, the resulting feature maps go through fully connected layers to produce the final output. Since both convolution and pooling are done with stride 1 and no padding, the size of the feature maps gets smaller at each step. This way, the network gradually captures more abstract and higher-level features (Analytics Vidhya, n.d.).

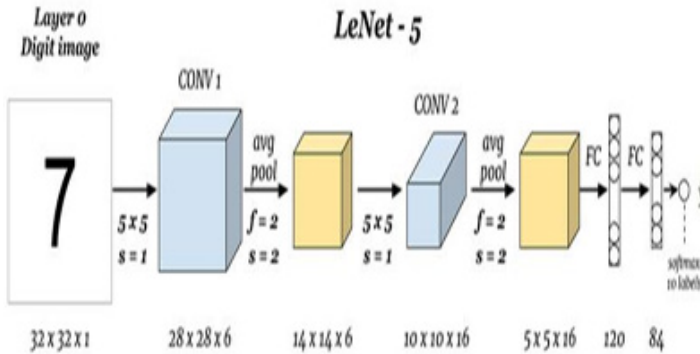


Fig 2. LeNet-5 Architecture (Analytics Vidhya, n.d.)

ResNet-50 Architecture

The ResNet50 network begins with a 7×7 convolutional layer with 64 filters and a stride of 2, followed by a 3×3 max pooling layer with stride 2. The first residual stage (Conv2_x) has three bottleneck blocks, each con-

taining 1×1 with 64 filters, 3×3 with 64 filters, and 1×1 with 256 filters. The second stage (Conv3_x) covers four blocks with 128, 128, and 512 filters in the same order. The third stage (Conv4_x) consists of six bottleneck blocks with 256, 256, and 1024 filters, and the final stage (Conv5_x) has three blocks with 512, 512, and 2048 filters. Finally, a global average pooling layer is applied, as shown in Fig. 4. (Analytics Vidhya, n.d.).

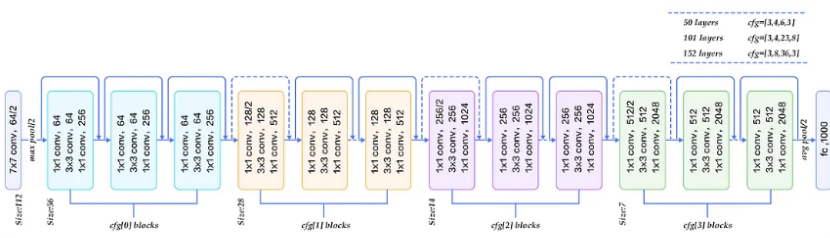


Fig 3. ResNet-50 Architecture (Analytics Vidhya, n.d.)

VGGNet Architecture

The extended version of AlexNet, called VGGNet, makes the network deeper, increasing it from 8 layers in AlexNet to 16–19 layers, while maintaining the quantity of parameters relatively low. Instead of using one 7×7 convolution filter, VGGNet uses a series of three 3×3 filters in each convolutional layer, as shown in Fig. 5. The network accepts input images of size $224 \times 224 \times 3$ (Elhassouny & Smarandache, 2019).

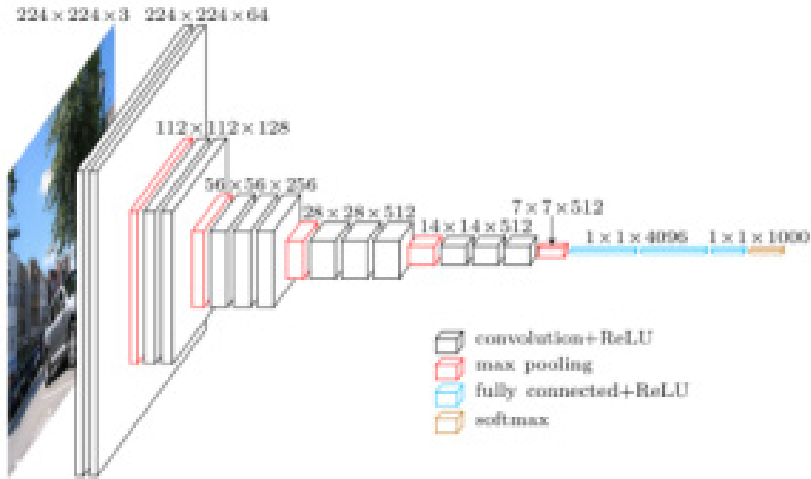


Fig 4. VGGNET Architecture (Elhassouny & Smarandache, 2019)

GoogLeNet/Inception Architecture

GoogleNet has 22 layers in total (excluding parameters). Its main component is the Inception module. This module applies different filter sizes in parallel within the same layer, including 1×1 , 3×3 , and 5×5 convolutions, along with 3×3 max pooling. The results from all these parallel filters are then combined into a single output, as shown in Fig. 6. The network usually takes input pictures of size $224 \times 224 \times 3$ (Elhassouny & Smarandache, 2019).

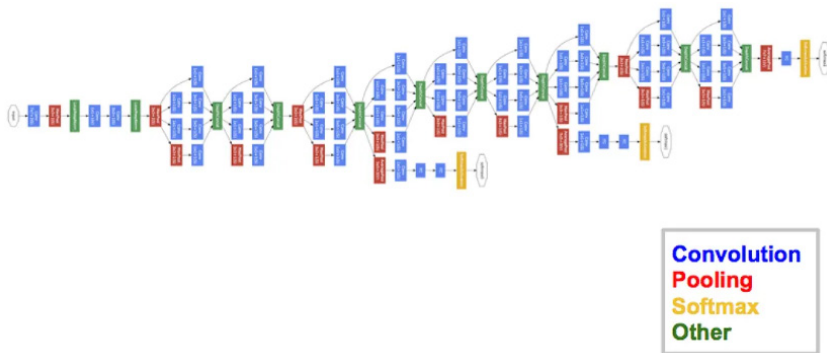


Fig 5. VGGNet Architecture (Elhassouny & Smarandache, 2019)

DenseNet Architecture

DenseNet begins with a 7x7 convolution layer, then moves on to max pooling, batch normalization, and ReLU activation. The network is composed of multiple dense blocks, with feature maps from all preceding layers being fed into each layer. Batch normalization, ReLU, a 1x1 bottleneck convolution, and a 3x3 convolution are all included in each dense layer, and the outputs are concatenated with the inputs. Transition layers reduce the size of the feature map between dense blocks by using 2x2 average pooling and 1x1 convolution. Lastly, a softmax layer generates the classification output following global average pooling, as illustrated in Fig. 7. Typically, the network accepts input images with dimensions of $224 \times 224 \times 3$ (Liu & Chen, 2021).

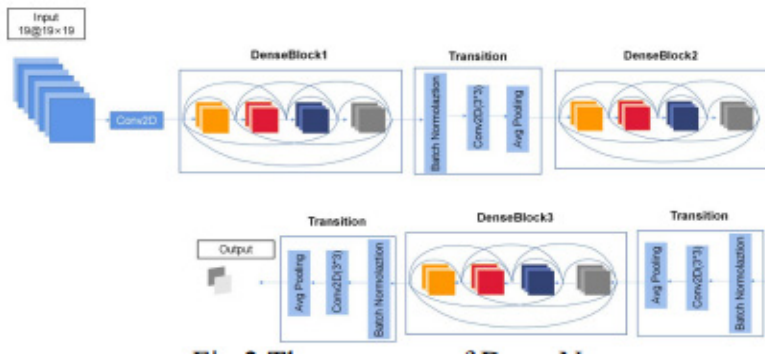


Fig 6. DenseNet Architecture (Liu & Chen, 2021)

YOLO Architecture

The YOLO architecture begins with an input layer that takes a fixed-size RGB image, usually $416 \times 416 \times 3$. In YOLOv3, the image is processed by a convolutional backbone called Darknet-53, which includes residual blocks, batch normalization, and Leaky ReLU activations (Ulhaq et al., 2021) to extract detailed feature maps. These features are then passed through the neck, where upsampling and concatenation combine multi-scale information. Lastly, for each anchor box at each grid cell, the prediction head outputs bounding boxes, objectness scores, and class probabilities. As illustrated in Fig. 8, Non-Maximum Suppression is used to refine the final output tensor of shape $S \times S \times [B(5+C)]$ in order to eliminate duplicate detections and retain only the most certain predictions (Ulhaq et al., 2021).

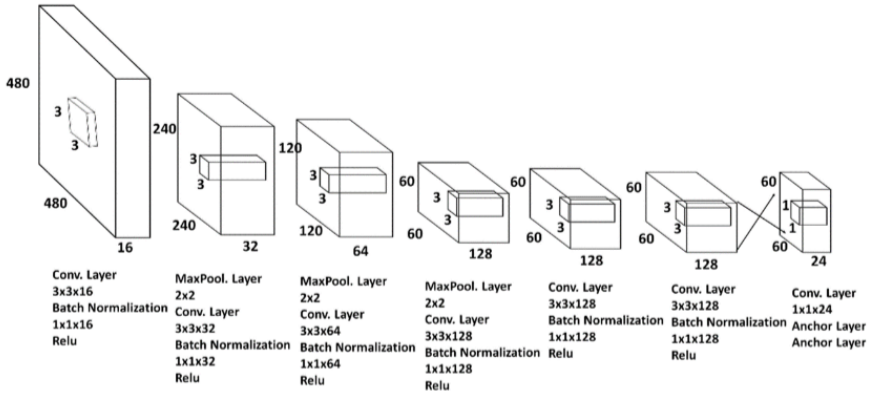


Fig 7. YOLO Architecture (Ulhaq et al., 2021)

SqueezeNet Architecture

SqueezeNet takes an input image of size 224×224×3 and processes it using fire modules, as shown in Fig. 9. With only 1.24 million parameters, it achieves high accuracy by mainly using 1×1 filters. Each fire module has a squeeze layer to reduce the number of channels and an expand layer with 1×1 and 3×3 filters, while postponing down-sampling to keep more spatial information.

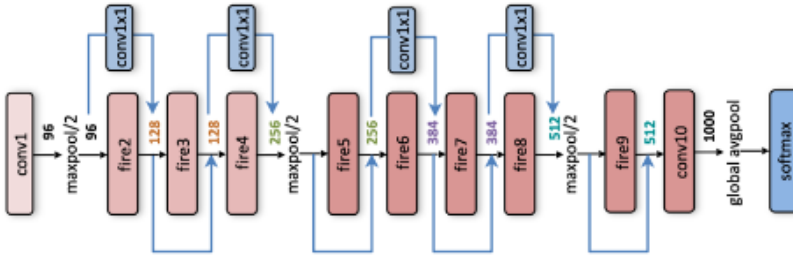


Fig 8. SqueezeNet Architecture (Elharrouss et al., 2022)

C) Evaluation Metrics

Various evaluation metrics are widely employed to measure classifier performance (Akinca et al., 2024). Equation 1 provides the accuracy, which is the percentage of accurate predictions among all of the model’s predictions (Dalianis, 2018).

$$Accuracy(Acc) = \frac{TP + TN}{TP + FP + TN + FN} \quad (1)$$

Recall is the percentage of real positive instances that are correctly identified, as shown in Equation 3, while precision is the fraction of instances predicted as positive that actually belong to the positive class, as shown in Equation 2(Dalianis, 2018).

$$Precision(P) = \frac{TP}{TP + FP} \quad (2)$$

$$Recall(R) = \frac{TP}{TP + FN} \quad (3)$$

The F1-score offers a fair evaluation of model performance, especially when handling false positives and false negatives. It is computed using Equation 4, which is the harmonic mean of precision and recall. True Positives (TP), True Negatives (TN), False Positives (FP), and False Negatives (FN), which indicate the numbers of accurate and inaccurate predictions for each class, are among the metrics that are obtained from the confusion matrix (Dalianis, 2018).

$$F_1 - score(F_1s) = 2 * \frac{Precision * Recall}{Precision + Recall} \quad (4)$$

D) Visulation of the Fault detection

As shown in Fig. 10, faults such as bird droppings and other surface contaminants can be effectively detected using deep learning-based methods which analyze the visual features of the images to distinguish between normal and faulty areas.

As illustrated in Figure 10, deep learning-based techniques may identify a broad range of issues in solar modules, from surface impurities like dust, bird droppings, and shadowing to structural flaws including cell fractures, cracks, and delamination. Without the requirement for manual feature engineering, these techniques distinguish between healthy and defective regions by automatically evaluating the visual features taken from module images. Cracks and other structural damages frequently show up as line-shaped flaws or discontinuities in the texture of the cells,

whereas surface-related problems usually show up as irregular patterns or localized intensity changes. Convolutional neural networks and other deep architectures may classify fault kinds accurately and robustly by learning these distinctive patterns. Furthermore, such automatic detection helps to optimize solar systems' long-term dependability, safety, and performance in addition to increasing diagnostic effectiveness and lowering the need for human intervention.



Fig 9. Failure detection of Solar panels (Kaggle, 2025)

REFERENCES

- Jalal, M., Khalil, I. U., & ul Haq, A. (2024). Deep learning approaches for visual faults diagnosis of photovoltaic systems: State-of-the-art review. *Results in Engineering*, 23, 102622.
- Kaggle. (2025, September). Datasets. <https://www.kaggle.com/datasets>
- Alatwi, A. M., Albalawi, H., Wadood, A., Anwar, H., & El-Hageen, H. M. (2024). Deep learning-based dust detection on solar panels: A low-cost sustainable solution for increased solar power generation. *Sustainability*, 16(19), 8664.
- Pathak, S. P., & Patil, S. A. (2023). Evaluation of effect of pre-processing techniques in solar panel fault detection. *IEEE Access*, 11, 72848–72860.
- Swapna, M., Sharma, Y. K., & Prasad, B. (2020). CNN architectures: AlexNet, LeNet, VGG, GoogleNet, ResNet. *International Journal of Recent Technology and Engineering*, 8(6), 953–960.
- Krizhevsky, A., Sutskever, I., & Hinton, G. E. (2012). ImageNet classification with deep convolutional neural networks. *Advances in Neural Information Processing Systems*, 25.
- Analytics Vidhya. (n.d.). CNNs architectures: LeNet, AlexNet, VGG, GoogleNet, ResNet and more. Medium. <https://medium.com/analytics-vidhya/cnns-architectures-lenet-alexnet-vgg-google-net-resnet-and-more-666091488df5>
- Hossain, M. B., Iqbal, S. H. S., Islam, M. M., Akhtar, M. N., & Sarker, I. H. (2022). Transfer learning with fine-tuned deep CNN ResNet50 model for classifying COVID-19 from chest X-ray images. *Informatics in Medicine Unlocked*, 30, 100916.
- Elhassouny, A., & Smarandache, F. (2019). Trends in deep convolutional neural networks architectures: A review. In 2019 International Conference of Computer Science and Renewable Energies (ICCSRE) (pp. 1–8).
- Liu, T., & Chen, T. (2021). A comparison of CNN and DenseNet for landslide detection. In 2021 IEEE International Geoscience and Remote Sensing Symposium (IGARSS) (pp. 8440–8443).
- Ulhaq, A., Adams, P., Cox, T. E., Khan, A., Low, T., & Paul, M. (2021). Automated detection of animals in low-resolution airborne thermal imagery. *Remote Sensing*, 13(16), 3276.
- Redmon, J., Divvala, S., Girshick, R., & Farhadi, A. (2016). You only look once: Unified, real-time object detection. In *Proceedings of the IEEE Conference on Computer Vision and Pattern Recognition* (pp. 779–788).
- Elharrouss, O., Akbari, Y., Almaadeed, N., & Al-Maadeed, S. (2022). Backbones-review: Feature extraction networks for deep learning and deep reinforcement learning approaches. *arXiv preprint arXiv:2206.08016*.
- Akinca, R., Firat, H., & Asker, M. E. (2024). Automated fault classification in solar panels using transfer learning with EfficientNet and ResNet models. *European Journal of Technique (EJT)*, 14(2), 164–173.
- Dalianis, H. (2018). Evaluation metrics and evaluation. In *Clinical Text Mining*:

Secondary Use of Electronic Patient Records (pp. 45–53). Springer.

Kaggle. (2025, September). CNN VGG16 used for solar panel fault detection.
<https://www.kaggle.com/code/pythonafroz/cnn-vgg16-used-for-solar-panel-fault-detection/notebook>

//

Chapter 3

INVESTIGATION OF SLOT PARAMETERS IN SYNCHRONOUS MOTOR DESIGN VIA FINITE ELEMENT METHOD AND MACHINE LEARNING APPROACHES

*İlyas ÖZER¹, Harun ÖZBAY²,
Adem DALCALI³*

1 Bandırma Onyedi Eylül University, Department of Computer Engineering, Bandırma.

2 Bandırma Onyedi Eylül University, Department of Electrical Engineering, Bandırma.

3 Bandırma Onyedi Eylül University, Department of Electrical and Electronics Engineering, Bandırma.

Introduction

Electric machines constitute one of the fundamental building blocks of modern engineering, playing an indispensable role in both daily life and in industrial and technological domains. Today, electrical energy is utilized across a wide spectrum ranging from industrial manufacturing facilities to transportation systems, from renewable energy plants to household technologies. One of the key driving forces behind this transformation is electric machines. By converting electrical energy into mechanical energy—or vice versa—they form the core of the modern world's energy infrastructure. For instance, motors used in industrial production lines determine the continuity and capacity of manufacturing processes, while generators in renewable energy plants enable the transfer of power generated from natural sources such as wind and hydroelectric systems to the grid. In smart home technologies, compact motors and actuators enhance comfort and automation, thereby transforming the overall user experience (Efe and Dalcalı, 2021).

In recent years, the rapid advancements in electric vehicle technologies have further increased the strategic importance of electric machines. Electric vehicles have become central to sustainable transportation solutions due to their near-zero emission levels, low operating costs, and high energy efficiency compared to conventional internal combustion vehicles. However, this technological transition has also reshaped the performance criteria expected from electric machines. While reliability and durability have traditionally been prioritized, electric vehicle drive systems now demand a combination of high-power density, high efficiency, quiet operation, low maintenance requirements, and compact design. In particular, the limited capacity of batteries has created a critical need for efficient energy utilization, making it essential for electric machines to operate with minimal energy losses during conversion processes (Özbay et al., 2020). In this context, permanent magnet synchronous machines (PMSMs) have emerged as one of the most prominent machine types in electric vehicle technologies and other advanced engineering applications. PMSMs can achieve high power density and high torque production through the use of strong permanent magnets mounted on the rotor surface. Moreover, their relatively simple structure, advantages in manufacturing, and ease of maintenance make these machines highly attractive. Compared to conventional induction motors, PMSMs offer superior efficiency, thereby directly contributing to the reduction of range anxiety in electric vehicles. This is because one of the most critical parameters in extending the distance that an electric vehicle can travel on a single charge is the minimization of energy conversion losses within the electric motor. However, the design of PMSMs also introduces several engineering challenges.

One of the most critical issues affecting their performance is torque ripple, particularly noticeable at low-speed operation. Among the various components contributing to torque ripple, the most well-known is the cogging torque. Cogging torque is an undesired torque component that arises from the interaction between the magnetic fields of the stator slots and the rotor-mounted permanent magnets. This torque, especially under low-speed or no-load conditions, can hinder smooth rotation, causing vibrations and oscillations. Consequently, minimizing cogging torque is of paramount importance in applications requiring high precision. A high level of cogging torque not only reduces the electromechanical performance of the motor but also introduces several secondary effects, most notably the problems associated with Noise, Vibration, and Harshness (NVH) (Dosiek and Pillay, 2007).

One of the most critical factors influencing the torque characteristics of PMSMs is the geometry of the stator slots. The stator structure constitutes one of the fundamental components of the magnetic circuit in an electric machine, and the uniformity of the magnetic flux distribution is directly dependent on its geometric configuration. In particular, the slot opening — located on the surface of the stator teeth facing the air gap — stands out as a key parameter that determines the electromagnetic behavior of the machine. The slot opening essentially defines the boundary conditions of the magnetic interaction between the stator and the rotor; therefore, even a minor geometric variation can lead to significant changes in the torque production characteristics of the machine. The width of the slot opening directly affects the distribution of magnetic flux density within the air gap. If the slot opening is excessively wide, the magnetic flux density between the stator teeth and the rotor magnets becomes unbalanced, leading to the generation of unwanted harmonic components. These harmonics, in turn, increase cogging torque. A high cogging torque level prevents smooth torque generation, particularly at low speeds, and intensifies vibration and noise. On the other hand, an overly narrow slot opening can also lead to adverse consequences. Extremely small openings complicate coil placement, making the assembly process more difficult. From an electromagnetic perspective, they may cause local magnetic saturation by concentrating flux density excessively, which not only increases losses but also adversely affects the overall efficiency of the machine (Dalcalı et al., 2020).

In addition to the slot opening, the geometry of the teeth tips is another factor that directly influences machine performance. The shape of the teeth tips can either smooth or sharpen the magnetic flux distribution within the air gap. For instance, rounded teeth tips help achieve a more uniform flux density distribution, whereas sharp-edged teeth tips

may lead to local magnetic concentrations. Therefore, when considered together, the slot opening and the teeth tip geometry play a decisive role in defining the electromagnetic behavior of the machine. Accordingly, during the electromagnetic design process, it is essential to evaluate all geometric parameters interactively rather than focusing solely on a single variable. The consequences of non-optimized slot openings are typically reflected in three main performance indicators: cogging torque, starting torque, and efficiency. High cogging torque prevents the machine from maintaining the desired torque smoothness, particularly at low speeds. A reduction in starting torque limits the machine's ability to initiate motion, which can cause serious performance issues in systems requiring high initial torque. The adverse effects on overall efficiency are more far-reaching; a decrease in efficiency directly translates into increased energy consumption. In electric vehicles, this leads to reduced driving range, while in industrial applications, it results in higher operating costs (Liu et al., 2024). At this point, accurate modeling and optimization of the slot opening hold great importance from an engineering perspective. In traditional approaches, designers have attempted to estimate these effects using analytical equations or a limited number of finite element analyses. However, with the recent advancements in computer-aided design and parametric modeling capabilities, it has become possible to investigate geometric parameters such as the slot opening within a much broader design space. This allows the effects of varying slot opening ratios on cogging torque, starting torque, and efficiency to be systematically examined, providing designers with the means to make more informed and data-driven design decisions (Dai et al., 2025).

A considerable number of studies in the literature have extensively investigated the effects of stator teeth tip geometry and slot opening parameters on the performance of PMSMs using different methodological approaches. The majority of these studies are based on conventional electromagnetic analysis techniques, employing analytical models and the Finite Element Method (FEM) to quantitatively assess the influence of various geometric variations on performance indicators such as torque ripple, magnetic flux distribution, air-gap flux density, harmonic content, magnetic losses, and eddy current and stray losses. In the study conducted by Yang et al., time-step FEM analyses demonstrated that reducing the slot opening suppresses inverter-induced harmonic flux components, resulting in a smoother air-gap flux density distribution and a reduction of up to 75% in magnet power losses. (Yang et al., 2022). In the study by Nair et al., the influence of stator teeth tips was investigated in terms of eddy current losses in the rotor magnets through 3D slot effect modeling. The analysis incorporated both analytical methods and FEM validation

(Nair et al., 2016). Furthermore, in the study conducted by Li et al., the interrelations between starting torque and torque ripple were quantitatively analyzed under different stator core types, teeth–pole combinations, and fully closed slot configurations. The adverse effects of local magnetic saturation conditions on torque smoothness and average torque were particularly emphasized (Li et al., 2018).

The strengths of such FEM and analytical models lie in their ability to represent magnetic circuit characteristics in detail, to reveal the influence of geometric features on magnetic saturation and air-gap flux distribution, and to enable the analysis of harmonic components. However, this approach also has certain limitations. In FEM analyses—particularly for 3D models—the need for high-resolution meshing, long computation times, and the requirement to analyze each combination of complex geometric variations individually present major challenges. This makes parameter scanning, optimization, or multi-objective design processes highly time-consuming and computationally expensive in wide design spaces. At this point, alternative approaches that have recently gained attention in the literature involve the use of Machine Learning (ML) and Artificial Intelligence (AI)-based surrogate models. These models, trained on simulation data, can rapidly predict performance outcomes for new combinations of geometric parameters in cases where conventional FEM analyses would otherwise require extensive computational effort. For example, in the study conducted by Farshbaf et al., a strategy called Waveform-Targeted Surrogate Modeling (WTSM) was introduced. Within this framework, comparative scenarios were examined using training–validation datasets, and it was demonstrated that the proposed method achieved higher computational efficiency in the overall optimization process compared to conventional Black Box Modeling (BBM) approaches (Roomi et al., 2022). Moreover, in the study conducted by Partovizadeh et al., a method was proposed in which dimensionality reduction was performed using the frequency components of torque signals under different geometric design variables, followed by the construction of a surrogate model through regression techniques. In this way, the periodic nature of the torque signal was preserved while the overall simulation cost was significantly reduced (Partovizadeh et al., 2025). The advantages offered by such ML/AI-based approaches can be summarized as follows:

- *Rapid prediction:* Once trained, surrogate models can generate results for new parameter combinations within seconds—or even milliseconds—without the need to run high-fidelity simulations such as FEM.
- *Extensive design-space exploration:* These models enable the si-

multaneous consideration of multiple geometric variables—such as slot opening, tooth tip inclination, tooth curvature, and coil placement—while supporting multi-parameter experimental designs (Design of Experiments, DOE).

- *Multi-objective optimization:* When multiple performance criteria—such as cogging torque, starting torque, efficiency, and losses—need to be evaluated simultaneously, ML-based models enable the rapid identification of Pareto-optimal solutions.
- *Uncertainty quantification:* Approaches capable of providing insights into model uncertainty (e.g., Gaussian Processes, Bayesian Neural Networks) allow the estimation of confidence intervals for FEM-based predictions. This is particularly valuable for analyzing the effects of manufacturing tolerances and variations in magnetic material properties.

Nevertheless, ML/AI approaches also have certain drawbacks and aspects that require careful consideration, such as the adequacy of the training dataset, the risk of overfitting, generalization capability, consistency with physical reality (e.g., magnetic saturation, harmonics), and the acceptability of prediction errors. Moreover, in some studies, the accuracy of ML-based surrogate models tends to decrease at extreme points or boundary conditions; therefore, such models are often employed in a hybrid framework alongside FEM simulations or experimental validation.

In this study, the effects of slot opening and slot height on cogging torque, starting torque, and efficiency in PMSMs are comprehensively investigated. A parametric simulation framework was first established, and datasets were generated for different slot opening and height configurations. Subsequently, the obtained data were processed using explainable machine learning models, resulting in a predictive mechanism that enables rapid estimations while maintaining engineering interpretability. Particularly through the use of SHapley Additive ExPlanations (SHAP)-based explainability techniques, the dominant influence of specific geometric parameters on various performance indicators was revealed in a transparent manner. One of the major engineering contributions of this approach is its ability to provide a guiding framework for decision-makers in multi-objective design problems. In practice, a designer seeks not only to minimize cogging torque but also to optimize both starting torque and efficiency. However, these three metrics inherently involve a trade-off relationship. For instance, while reducing the slot opening may lower cogging torque, it can simultaneously have adverse effects on efficiency or starting torque. Therefore, achieving an optimal balance within the

design process requires not only numerical analysis but also data-driven decision support systems.

Designed Motor and Its Characteristics

PMSMs have shown remarkable advancements, particularly due to progress in power electronics and high-performance magnetic materials. These machines are especially preferred in applications involving low rotational speeds and variable-speed operation. The primary reason is their ability to maintain key performance parameters—such as efficiency and power factor— independent of the rotational speed. In permanent magnet machines, the magnets continuously supply magnetic flux to the magnetic circuit, thereby generating the rotor’s magnetic field. The magnets employed in such systems are expected to possess a wide hysteresis loop, high coercive force, and strong residual magnetization (Galioto et al., 2014). Ceramic, Alnico, SmCo, and NdFeB magnets are widely used in various industrial machine applications. Although Alnico magnets exhibit high thermal stability, they are brittle in nature and can be easily demagnetized. Ceramic magnets, on the other hand, have a relatively low maximum energy product. In electrical machines, the primary objective is to achieve the highest possible power output within the smallest possible volume. NdFeB magnets, which are based on rare-earth elements, offer exceptionally high-power density even in compact structures due to their high maximum energy product (BH_{max}) (Zhang et al., 2022; Dalcali et al., 2020). For this purpose, a surface-mounted, four-pole PMSM utilizing NdFeB-type magnets was investigated in this study. The specifications of the motor analyzed are presented in Table 1.

Table 1. *Design parameters of the proposed motor*

Parameter	Value	Parameter	Value
Rated power (kW)	10	Stack length	100
Number of poles	4	Number of slots	24
Stator outer diameter (mm)	275	Stator / Rotor material	M19
Rotor outer diameter (mm)	154.8	Magnet material	N36

Figure 1 presents the model of the initial motor design and the mesh structure used in the finite element analysis.

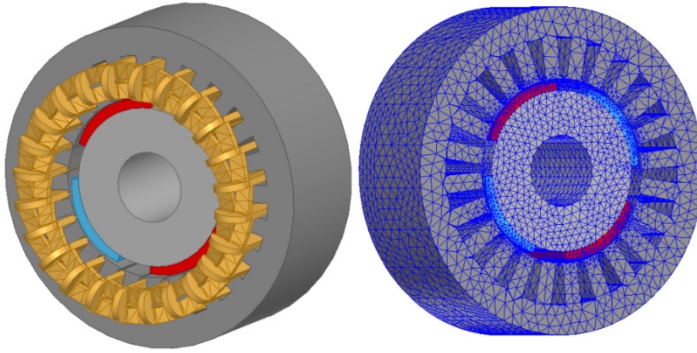


Figure 1. Geometric model and meshing structure of the PMSM.

The analysis of electrical machines is a complex process that requires multidisciplinary and interconnected solutions. The FEM is one of the most widely used and effective numerical approaches for solving such problems. By creating 2D or 3D models of the machine using FEM, performance outputs such as flux density distribution, voltage waveforms, loss profiles, and torque variations can be obtained with high accuracy. The implementation of this method not only enables precise determination of design parameters but also offers significant advantages in terms of time and cost efficiency during the design process. The fundamental performance parameters of the motor under rated load and no-load operating conditions are presented in Table 2.

Table 2. Fundamental performance of the designed PMSM under rated and no-load condition

	Parameter	Value
Rated load	Output power (W)	10001
	Efficiency (%)	91.09
	Rated torque (Nm)	53.06
No-load	Cogging torque (Nm)	0.418
	Stator teeth flux density (T)	1.561
	Stator yoke flux density (T)	1.613
	Total weight (kg)	42.301
	Slot fill factor (%)	61.94

At rated load, the motor produces approximately 10 kW of output power with a notably high efficiency of 91.09%. The nominal torque value

was obtained as 53.06 Nm, indicating that the motor can operate stably in low-speed applications. Under no-load conditions, the measured cogging torque of 0.418 Nm demonstrates that the motor provides a smooth and vibration-free torque profile. The stator tooth flux density was determined to be 1.561 T, while the stator yoke flux density reached 1.613 T; these values indicate a well-balanced magnetic circuit operating within the optimal region, without approaching material saturation limits. Furthermore, the total weight of the motor is 42.301 kg, which reflects a compact structure relative to the generated power. The slot fill factor of 61.94% shows that the windings are efficiently placed within the slots, ensuring effective utilization of copper.

The magnetic flux distribution obtained under nominal load conditions is presented in Figure 2. Examination of the flux density distribution reveals that, as expected, the highest concentrations occur in the stator teeth. Moreover, considering the BH characteristics of the M19 core material, a homogeneous and well-balanced flux distribution is achieved throughout the motor. The flux density in the yoke region remains within acceptable limits, indicating that magnetic saturation has not been reached.

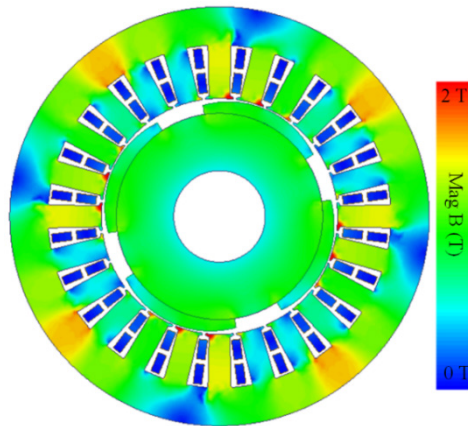


Figure 2. Magnetic flux density distribution of the designed PMSM.

Another critical parameter that must be considered in motor design is the cogging torque value. This torque arises from the magnetic interaction between the magnets providing the rotor flux and the stator, leading to noise and vibration during motor operation (Zhao et al., 2024). The cogging torque can be expressed as a function of the reluctance, air-gap flux, and rotor position, as given in Equation 1 (Dosiak and Pillay, 2007).

$$T_{vuruntu} = \frac{1}{2} \Phi_g^2 \frac{d\mathcal{R}}{d\theta} \quad (1)$$

As can be seen from Equation 1, any modification in the air-gap geometry directly affects the cogging torque of the motor. The variation of cogging torque with respect to rotor position for the initial design is presented in Figure 3.

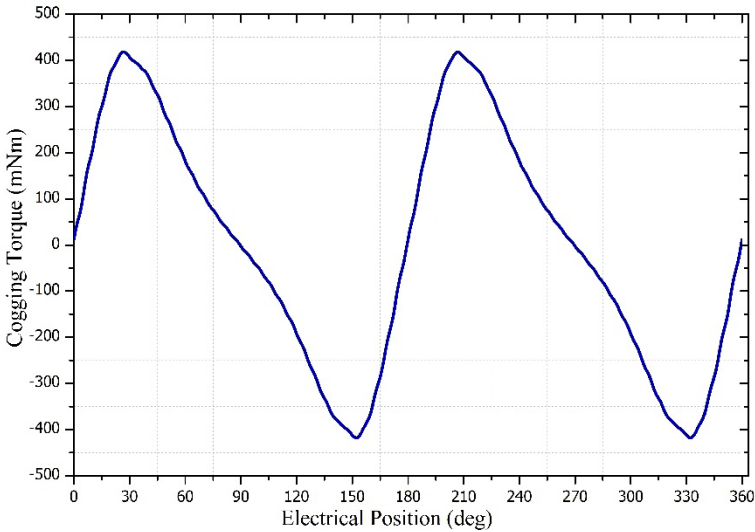


Figure 3. Variation of cogging torque with rotor position for the initial motor design.

Design of Experiments

In synchronous machines, the rotor and stator slot geometries significantly influence critical design parameters such as electromagnetic performance, efficiency, and generated torque (Jia et al., 2015). For this purpose, the effect of the stator slot structure on performance was examined in two stages. In the first stage, the influence of slot width (B_{s0} , B_{s1} , and B_{s2}) was analyzed, and in the second stage, the effect of slot height (H_{s0} , H_{s1} , and H_{s2}) was investigated. The slot structure and the variables used in this analysis are illustrated in Figure 4.

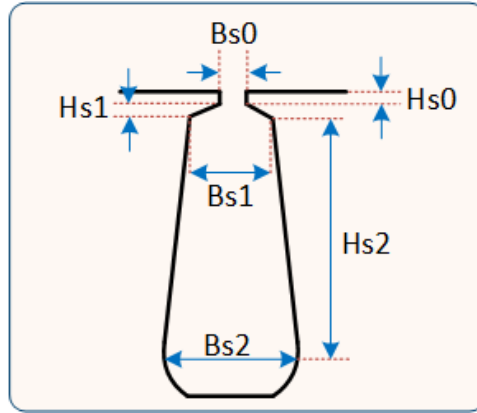


Figure 4. Stator slot structure and geometrical parameters used in the analysis.

The parameters presented in Table 3 define the fundamental variables and limits used to characterize the stator slot geometry of the motor. Variations in slot width and height directly affect magnetic flux distribution, leakage inductance, torque generation, and thermal behavior. Therefore, considering these variables in optimization studies is of great importance for improving the motor’s efficiency, torque ripple characteristics, and overall loss performance. According to the defined conditions, a total of 25641 configurations were generated for the first stage and 19844 configurations for the second stage. For each configuration, the output power, induced torque, cogging torque, efficiency, slot fill factor, total weight, and stator teeth flux density parameters of the motor were analyzed.

Tabl3 3. Design variables and boundary limits used for defining the stator slot geometry

Variable	Lower limit (mm)	Upper limit (mm)	Resolution (mm)
Bs0	0.5	3	0.125
Bs1	2	10	0.25
Bs2	2	20	0.5
Hs0	0.1	2.2	0.1
Hs1	0.1	2.2	0.1
Hs2	22	42	0.5

Generated Datasets

Two separate parametric scanning datasets were employed in this study. The BS dataset investigates the influence of the slot width family, while the HS dataset examines the effect of slot height. Both datasets consist of simulation records generated from the parametric model, where each row corresponds to the evaluation results of a unique stator-rotor geometry configuration. The data entries include both input columns—representing geometric and operating parameters—and multiple output columns, thereby enabling the simultaneous modeling of multiple target variables with a single predictor. In accordance with the design framework detailed in the previous sections, the BS dataset specifically explores variables related to slot width (bs0, bs1, bs2), whereas the HS dataset systematically scans slot height parameters (hs0, hs1, hs2). The design space and experimental size are consistent with the boundary and step values defined in the Design of Experiments section of this chapter. Therefore, the datasets presented here directly constitute the data foundation for the performance tables and figures reported in the same section.

The key input parameters of the model are the slot width variables (bs0, bs1, bs2) and the slot height variables (hs0, hs1, hs2). Six primary output parameters were defined: output power, cogging torque, rated torque, efficiency, stator teeth flux density, and slot fill factor. These targets represent the three main axes of design decisions in terms of drive performance, NVH characteristics, and electromagnetic feasibility. Therefore, their simultaneous prediction within a unified modeling framework significantly accelerates the multi-objective design decision process. The performance metrics and their relative importance rankings are fundamentally based on these six targets and are fully consistent with the structural content of the datasets.

The BS dataset consists of 25,641 rows and 11 columns. Each row represents the results of a geometry combination belonging to the slot width family, while six output columns correspond to the target variables and the remaining columns define the design parameters. In this dataset, the parameters bs0, bs1, and bs2 play a dominant role. The scanning range for the bs2 variable is between 2 and 20 mm, with an average sample value of approximately 11 mm. Since the number of rows containing valid target values is very close to the total number of samples, sufficient density and balance are achieved for multi-output regression analyses.

The HS dataset is organized into 19,844 rows and 11 columns. In this dataset, the parameters forming the slot height family—hs0, hs1, and hs2—were independently varied. Specifically, the hs2 variable ranges be-

tween 22 and 42 mm, with an average value of approximately 32 mm. Similar to the BS dataset, the HS dataset also contains six target columns, and each row represents a unique slot geometry configuration. The scope and resolution are consistent with the defined experimental design, ensuring sufficient density for model training and enabling the generation of reliable validation statistics for each target variable.

Together, these two datasets form the foundation of the performance and importance analyses presented in the results section: the BS dataset quantitatively captures the influence of slot width, while the HS dataset reveals the impact of slot height on motor performance.

Modeling Methodology Framework

In this study, the effect of slot geometry on the electromagnetic performance of surface-mounted PMSMs was investigated using a supervised surrogate model constructed from high-resolution numerical experiment results. ML is a general-purpose approach that has been successfully applied in various domains, including speech processing (Özer et al., 2018a; Özer et al., 2017), biomedical signal processing (Görür et al., 2023; Özer et al., 2023), and natural language processing (Özer et al., 2018b). In this approach, the design variables are taken as inputs, and a multi-output regression model is trained to learn the mapping from these variables to the target vector. In this way, instead of relying on computationally expensive simulations, a fast and interpretable predictive tool is developed that can be used online during the design process.

For the machine, the design space is defined as $x \in \mathbb{R}^p$, while the performance outputs are represented as $y \in \mathbb{R}^6$. The target vector comprises output power, cogging torque, rated torque, efficiency, stator tooth flux density, total weight, and slot fill factor. The objective is to learn a function $h_\theta: \mathbb{R}^p \rightarrow \mathbb{R}^6$ that minimizes the expected loss function. The loss is evaluated using a metric that accounts for multi-output errors and combines mean squared error with explained variance. For performance reporting, the coefficients of determination (R^2), mean absolute error (MAE), and root mean square error (RMSE) are employed.

In this study, an ensemble model based on gradient-boosted decision trees was employed as the primary learner. A separate gradient boosting process was applied for each target variable, while the multi-output structure was established through a wrapper framework. This configuration achieved a balanced trade-off between accuracy and interpretability by capturing nonlinear relationships, local saturation effects, and scale variations among targets. The model was trained with standard regularization and statistical balance to prevent overfitting of parameters, result-

ing in a reliable model that can generalize across different design regions. The overall performance was evaluated using a k-fold cross-validation scheme. In the five-fold setup, the training and validation sets were resampled in each iteration, and the mean and standard deviation of the R^2 , MAE, and RMSE metrics were reported for each target. For assessing the average performance of the multi-output model, a variance-weighted R^2 metric was adopted. This approach not only reflects the mean predictive accuracy but also quantifies the model's stability across the design space, making the relative difficulty of certain targets more discernible.

The influence of input variables on the model was examined using a permutation-based importance analysis method. After randomly shuffling each input column, the resulting decrease in explained variance (ΔR^2) was computed, where this reduction indicates the importance of the corresponding variable. Repeated permutations ($n=50$) were performed to reduce uncertainty, and the standard deviations of the importance values were reported. This model-agnostic approach is directly linked to the performance metric and allows for comparison across different learning models. The resulting importance ranking clearly demonstrates the dominant role of scale parameters and the varying influence of slot dimensions on different target variables.

The model outputs are visually validated for each target through actual-predicted distribution plots. The degree of clustering around the 45-degree reference line is evaluated together with the R^2 , RMSE and normalized RMSE metrics. These visualizations provide insights beyond average performance metrics, allowing the identification of regions within the design space where deviations become more significant or where systematic bias emerges. Consequently, the targets that require either aggressive or cautious optimization can be distinguished, and local validation regions can be selected accordingly.

The multi-output structure enhances data efficiency by enabling the sharing of common input patterns among targets. Cross-validation and repeated permutation analyses are sensitive to variations arising from randomness, and the reported standard deviations quantitatively represent this uncertainty. In cases where strong correlations exist among variables, importance scores may be distributed across correlated features; therefore, complementary analyses using partial dependence plots or SHAP-based local explanations are conducted. This ensures that both global trends and local effects are consistently interpreted within the same methodological framework.

The proposed framework is trained using knowledge derived from

high-cost discrete simulations and provides a surrogate model capable of generating responses within milliseconds during deployment. In the design process, the search space is stratified according to the importance ranking of the variables: scale parameters are fixed within narrow ranges or constrained through coarse scans, followed by systematic sweeps across the most influential slot dimensions. Confidence margins for each target are defined using normalized error profiles, and additional validation steps are incorporated at critical thresholds. This process enables rapid design iterations and reliable decision support in engineering applications where electromagnetic performance must be evaluated in conjunction with NVH and efficiency constraints. The proposed methodology is based on a streamlined approach that integrates key components such as uniform data representation, multi-output gradient boosting, cross-validation, permutation-based explainability, and target-specific consistency checks. This structure is scalable for expanding design spaces and increasing data volumes, and can be further extended with hyperparameter optimization, ensemble diversification, or region-specific modeling when necessary. Consequently, it provides a reliable, fast, and interpretable modeling framework for addressing electromagnetics-oriented design problems.

Results and Discussion

The results presented in Table 4 demonstrate that the model predicts the outputs with exceptionally high accuracy for both the BS and HS datasets. An R^2 value of 0.999 indicates that the model explains nearly all of the total variance, while the low MAE and RMSE values show that the prediction errors remain minimal in both absolute and root-mean-square terms. The smaller MAE and RMSE observed in the HS dataset compared to the BS dataset suggest that the relationships within this design space may be more regular or that the simulation noise is relatively lower. This level of accuracy confirms that the proposed model can be reliably utilized for rapid design exploration, sensitivity analysis, and preliminary optimization studies.

However, the overall metrics presented in Table 4 should be interpreted with contextual considerations during the decision-making process. Particularly for performance targets sensitive to operating conditions—such as power and torque—the error distribution may broaden within certain local regions. Therefore, when making design decisions near critical thresholds, it is advisable to define safety margins and perform a limited number of additional simulations for local validation to ensure more reliable outcomes. Such an approach enables the use of high average accuracy in a balanced manner, integrating risk management and engi-

neering assurance.

Table 4. Overall prediction performance metrics of the proposed model for BS and HS datasets

Dataset	R ²	MAE	RMSE
BS	0.999414	0.143784	0.382614
HS	0.999608	0.034192	0.099394

The permutation-based importance ranking presented in Table 5 reveals the clear dominance of the Total Net Weight variable in both datasets. This finding quantitatively confirms the primary influence of machine scaling and magnetic circuit sizing on power, torque, efficiency, and flux-related indicators. In the BS dataset, the variables *bs0* and *bs1*, which represent the slot opening and width, rank among the top contributors—indicating the strong influence of air-gap reluctance and leakage flux mechanisms. Conversely, in the HS dataset, the prominence of the height family variables *hs0*, *hs2*, and *hs1* suggests that tooth–slot saturation and flux distribution are the principal mechanisms governing the performance targets.

The obtained results necessitate a hierarchical prioritization strategy in the design process. In the first stage, scaling parameters should be defined within narrow bounds or explored through a coarse search; subsequently, the main slot dimensions that exhibit more consistent relationships with the target metrics should be examined in detail through systematic analyses. On the BS side, the relatively low importance of *bs2* may indicate a limited marginal contribution within the current sample; however, since correlations among variables can lead to the redistribution of importance scores, it would be appropriate to support this interpretation with local explainability tools such as partial dependence plots, Individual Conditional Expectation (ICE), or SHAP analyses. In practice, this hierarchical structure directly guides the planning of design exploration and optimization stages—starting with scale parameters, followed by critical slot dimensions, and finally secondary geometric or operational adjustments.

Table 5. *Permutation-Based Feature Importance (n = 50 Repetitions)*

Variable	Rank	Feature	Importance (mean)	Importance (std)
BS	1	Total Net Weight	1.1075	0.0054
BS	2	bs0	0.7086	0.0041
BS	3	bs1	0.5087	0.0036
BS	4	bs2	0.0101	0.0001
HS	1	Total Net Weight	1.3342	0.0089
HS	2	hs0	0.601	0.0045
HS	3	hs2	0.396	0.0027
HS	4	hs1	0.193	0.0017

The permutation importance analysis performed for both datasets clearly reveals the dominant factors that govern the design behavior. As illustrated in Figure 5, the Total Net Weight exhibits the highest importance score in the BS dataset, followed by bs0 and bs1, indicating that scale and slot width parameters exert a strong influence on the output metrics. The comparatively lower importance of bs2 suggests that its contribution may be limited or that its importance score may have been shared with other width-related variables due to inter-variable correlations.

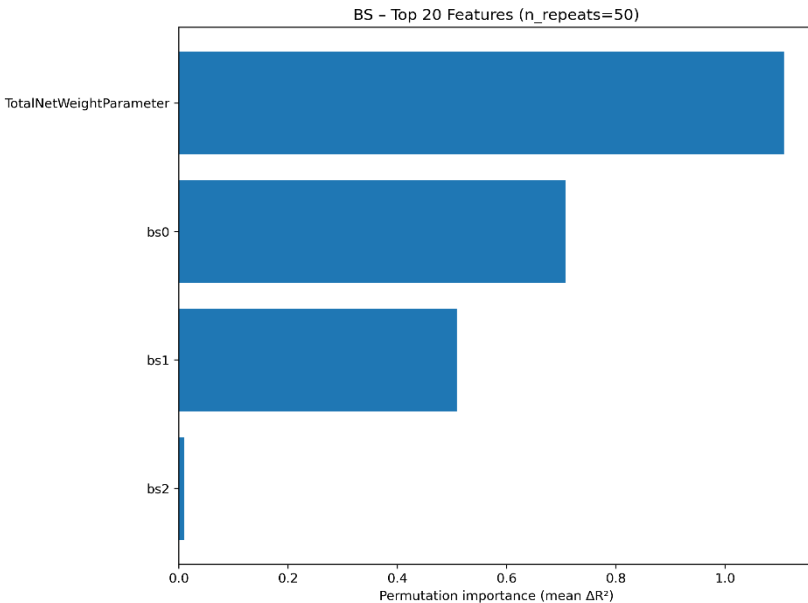


Figure 5. *Feature importance score for BS dataset.*

Figure 6 shows that, on the HS side, the height-related variables (hs0, hs2, hs1) emerge as dominant contributors. While the scale indicator, Total Net Weight, remains at the top of the ranking, the different height parameters play a decisive role in determining the outputs through mechanisms such as flux distribution, magnetic reluctance, and saturation. When Figures 5 and 6 are considered together, it becomes evident that the slot opening/width parameters are critical for the BS dataset, whereas the height parameters dominate in the HS dataset; in both cases, the scale factor—represented by the total net weight—acts as the primary determinant of overall performance.

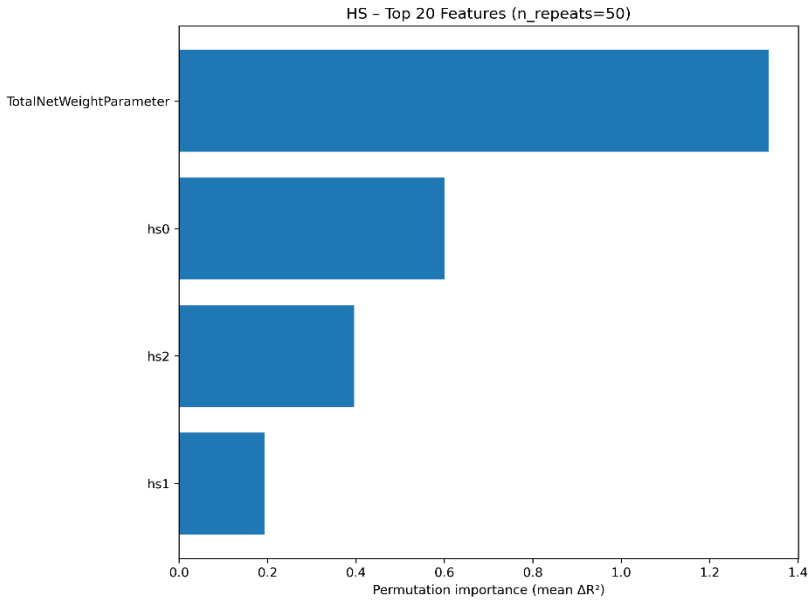


Figure 6. Feature importance score for HS dataset.

Interpreting the model's goodness-of-fit distributions for each target in conjunction with this hierarchy provides a more robust design guidance. As shown in Figure 7, the target-based R^2 values for the BS dataset indicate an almost perfect agreement in variables such as cogging torque, stator tooth flux density, and slot fill factor. On the other hand, the relatively lower R^2 values observed for power and nominal torque are consistent with the results presented in Table 4.

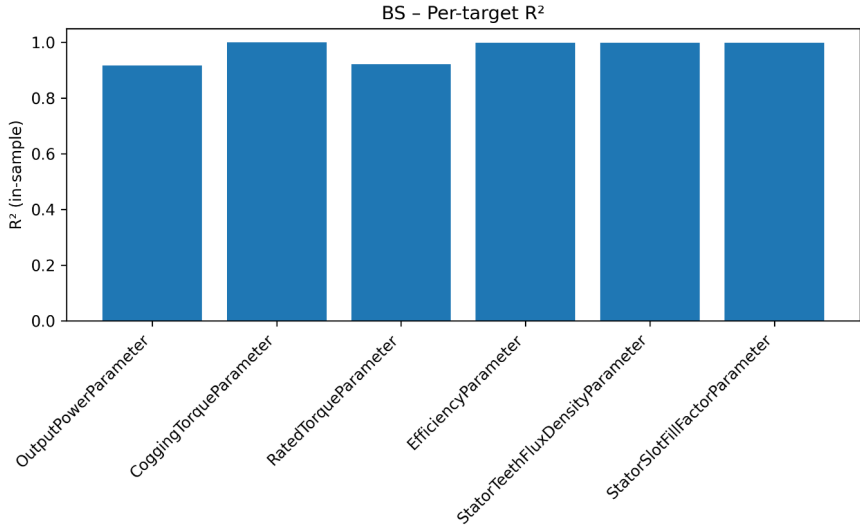


Figure 7. R^2 scores for BS dataset.

As shown in Figure 8, the R^2 values for the HS dataset remain generally high; however, the distributions for power and nominal torque appear more compact, indicating that the model exhibits a more stable performance for these targets compared to the BS dataset. This distinction supports the earlier observation that the relationships between targets and design variables are more uniform within the HS design space, or that the data noise is relatively lower. The visual comparison of R^2 values provides a practical guide for determining which targets can be optimized with greater confidence; for instance, a higher R^2 in torque-related variables sensitive to NVH implies a more reliable basis for sensitivity analysis.

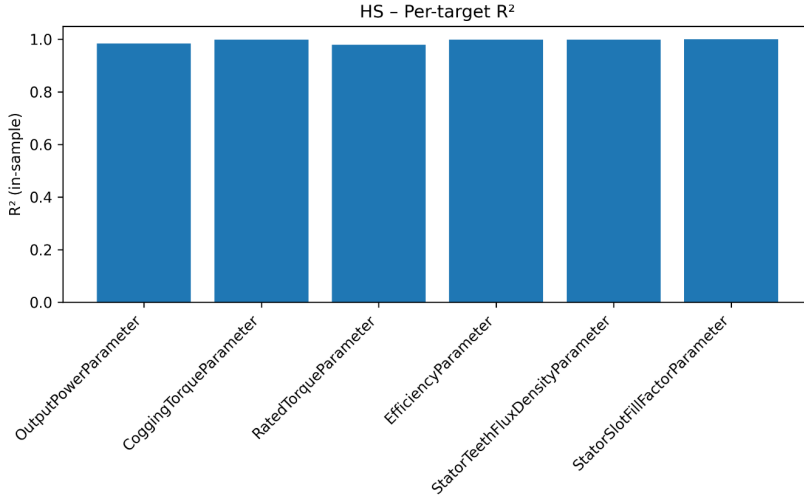


Figure 8. R^2 scores for HS dataset.

The nRMSE chart for the BS dataset, presented in Figure 9, reveals that the errors are relatively higher for the power and nominal torque targets. This finding indicates that these objectives are more sensitive to non-geometric operating conditions, such as speed or winding parameters. Conversely, the low nRMSE values observed for cogging torque and stator tooth flux density reaffirm that geometric parameters are the dominant influencing factors for these targets.

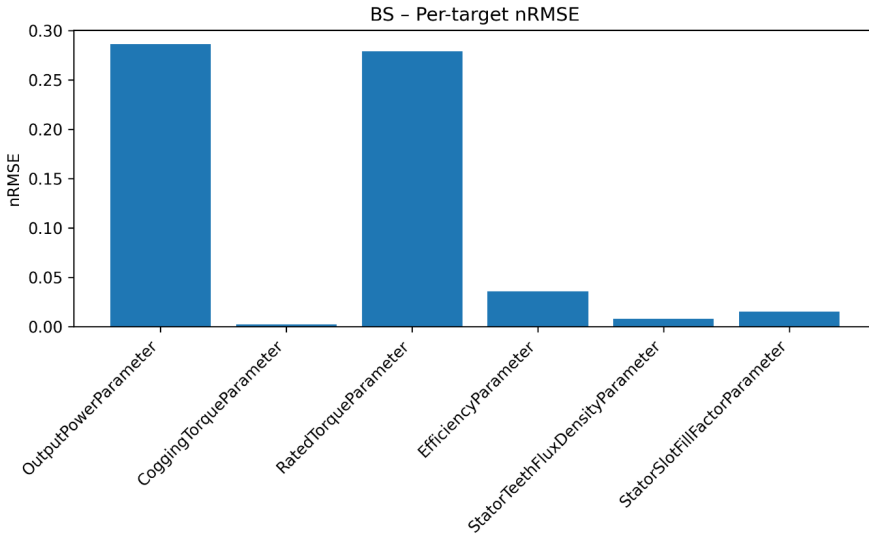


Figure 9. nRMSE scores for the BS dataset.

The nRMSE profile of the HS dataset shown in Figure 10 exhibits a tighter distribution, consistent with the R^2 observations, and indicates better control over power and nominal torque outputs. The comparison between the two datasets highlights the necessity of defining confidence margins on a target-specific basis: while aggressive parameter variations may be acceptable for targets with low nRMSE values, a more cautious and validation-oriented approach should be adopted for those with higher nRMSE levels.

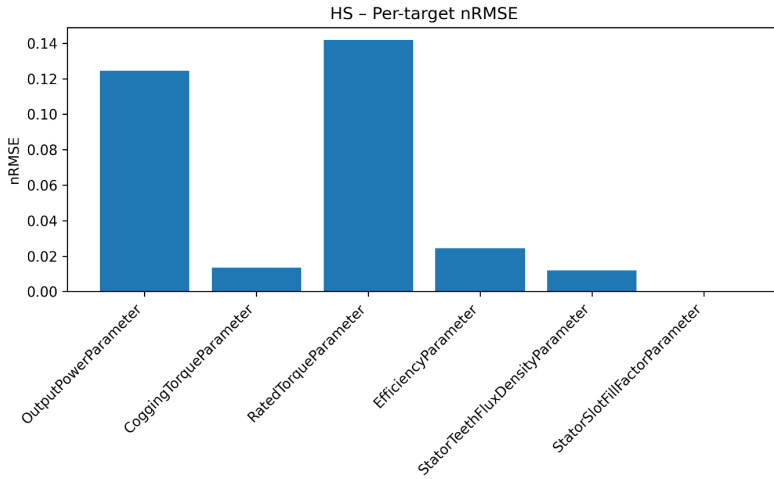


Figure 10. nRMSE scores for the HS dataset.

Figures 11 and 12 present the actual–predicted scatter plots. In Figure 11, the scatter for the BS dataset corresponding to the power output is concentrated around the 45° reference line, although it exhibits a relatively wider spread compared to other targets. The R^2 , RMSE, and nRMSE values reported in the figure title quantitatively support this observation, in full agreement with the results presented in Table 4 and the corresponding performance graphs.

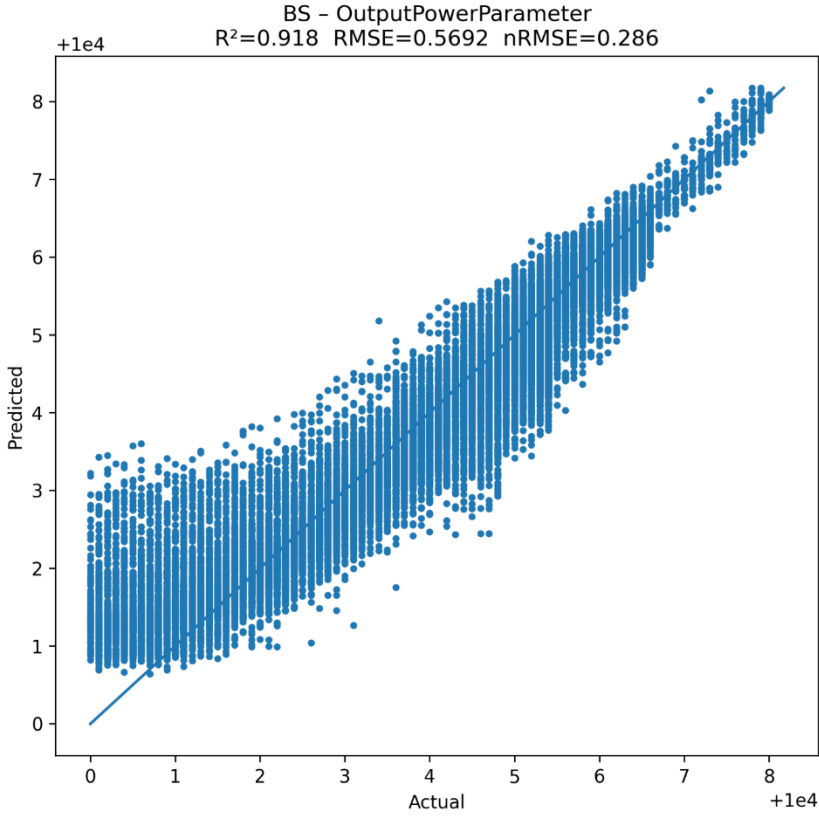


Figure 11. Actual–predicted scatter plot for the BS dataset (Output Power).

In Figure 12, the scatter corresponding to the power target in the HS dataset exhibits a tighter clustering, indicating more stable and predictable design iterations. When Figures 11 and 12 are evaluated together, it becomes evident that for the power target, a more aggressive design exploration strategy is suitable for the HS configuration, whereas a cautious, validation-supported approach is more appropriate for the BS configuration.

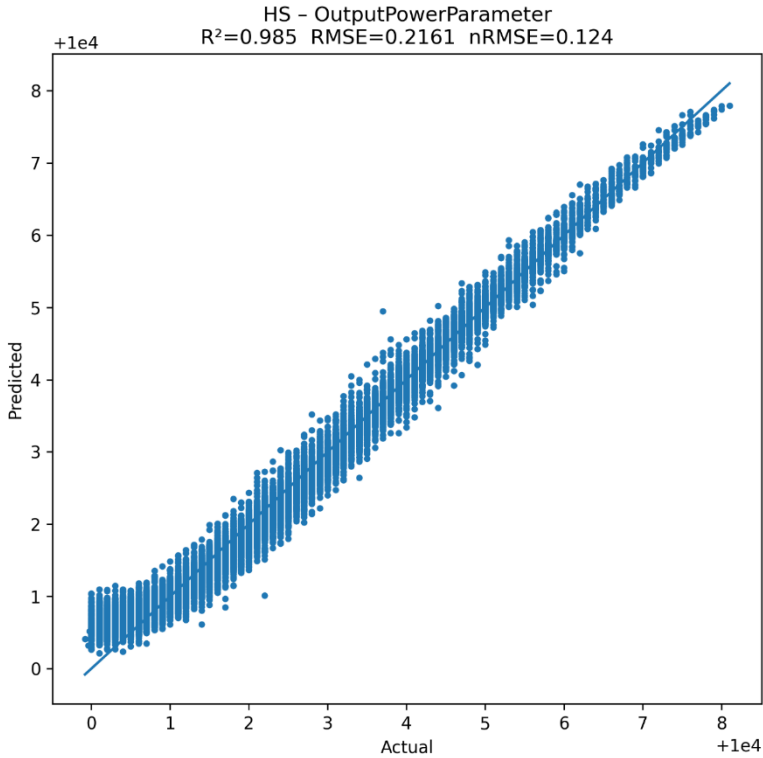


Figure 12. Actual–predicted scatter plot for the HS dataset (Output Power).

The results indicate that the design space should be approached in a hierarchical manner. In the first stage, scale parameters should be fixed or explored within narrow ranges according to the permutation-based importance rankings. Subsequently, critical slot dimensions—such as bs0 and bs1 for the BS dataset, and hs0 and hs2 for the HS dataset—should be systematically swept. At this stage, R^2 and nRMSE results can be used as guidance for target-specific selection: while wide-range explorations with sparse sampling are suitable for targets such as efficiency and flux density, which exhibit high accuracy and low error, denser sampling and localized refinement are required for more complex targets such as power and torque. This approach accelerates both the experimental design and optimization processes, enabling rapid progress in well-behaved targets while ensuring reliable steps for the more challenging ones.

References

- Dai, L., Niu, S., Gao, J., Liu, K., Huang, S., & Chan, W. L. (2025). Diverse slot-opening designs for cogging torque and performance optimization in PM machines. *IEEE Transactions on Transportation Electrification*, 11(3), pp. 8414-8426.
- Dalcalı, A., Kurt, E., Çelik, E., & Öztürk, N. (2020). Cogging torque minimization using skewed and separated magnet geometries. *Journal of Polytechnic*, 23(1), 223–230.
- Dosiek, L., & Pillay, P. (2007). Cogging torque reduction in permanent magnet machines. *IEEE Transactions on Industry Applications*, 43(6), 1565-1571.
- Efe, S.B., & Dalcalı, A. (2021). Harmonic and Inter-Harmonic Analysis in Electric Machines. *Electronic Letters on Science and Engineering*, 17(2), 117-125.
- Farshbaf Roomi, F., Vahedi, A., & Nobahari, A. (2022). Electrical machines surrogate-based design optimization based on novel waveform targeting strategy with improvement of the computational efficiency. *IET Electric Power Applications*, 16(11), 1286-1299.
- Galioto, S. J., Reddy, P. B., El-Refaie, A. M., & Alexander, J. P. (2014). Effect of magnet types on performance of high-speed spoke interior-permanent-magnet machines designed for traction applications. *IEEE Transactions on Industry Applications*, 51(3), 2148–2160.
- Gorur, K., Olmez, E., Ozer, Z., & Cetin, O. (2023). EEG-driven biometric authentication for investigation of Fourier synchrosqueezed transform-ICA robust framework. *Arabian Journal for Science and Engineering*, 48(8), 10901-10923.
- Jia, S., Qu, R., & Li, J. (2015). Design considerations and parameter optimization of stator wound field synchronous machines based on magnetic the gear effect. In *Proceedings of the 2015 IEEE Energy Conversion Congress and Exposition (ECCE)*, 5195-5202.
- Li, Y., Zhu, Z. Q., & Li, G. J. (2018). Influence of stator topologies on average torque and torque ripple of fractional-slot SPM machines with fully closed slots. *IEEE Transactions on Industry Applications*, 54(3), 2151-2164.
- Liu, F., Liu, J., & Yang, Y. (2024). An Optimization Design for Reducing Cogging Torque in Permanent Magnet Synchronous Motors. In *Proceedings of the 2024 27th International Conference on Electrical Machines and Systems (ICEMS)* pp. 156-161.
- Nair, S. S., Chen, L., Wang, J., Chin, R., Manolas, I., & Svehkarenko, D. (2016). 3D analytical slotting-effect model for magnet loss prediction in SPM machines. In *Proceedings of the 8th IET International Conference on Power Electronics, Machines and Drives (PEMD)*, IET.
- Özbay, H., Közkurt, C., Dalcalı, A., & Tektaş, M. (2020). Geleceğin ulaşım tercihi: Elektrikli araçlar. *Journal of Intelligent Transportation Systems and Applications*, 3(1), 34-50.
- Özer, Z., Cetin, O., Görür, K., & Temurtaş, F. (2023). Brain decoding over the MEG signals using Riemannian approach and machine learning. *Balkan*

Journal of Electrical and Computer Engineering, 11(3), 207-218.

- Özer, I., Ozer, Z., & Findik, O. (2017). Lanczos kernel based spectrogram image features for sound classification. *Procedia Computer Science*, 111, 137-144.
- Özer, I., Ozer, Z., & Findik, O. (2018a). Noise robust sound event classification with convolutional neural network. *Neurocomputing*, 272, 505-512.
- Özer, Z., Ozer, I., & Findik, O. (2018b). Diacritic restoration of Turkish tweets with word2vec. *Engineering Science and Technology, an International Journal*, 21(6), 1120-1127.
- Partovizadeh, A., Schöps, S., & Loukrezis, D. (2025). Fourier-enhanced reduced-order surrogate modeling for uncertainty quantification in electric machine design. *Engineering with Computers*, 1-21.
- Yang, G., Wang, X., Yang, C., Wang, D., Wu, H., & Wang, X. (2022). Effect of slot opening on permanent magnet power loss of a permanent magnet synchronous machine driven by PWM. *Energies*, 15(20), 7485.
- Zhang, Y., Zhao, C., Dai, B., & Li, Z. (2022). Dynamic Simulation of Permanent Magnet Synchronous Motor (PMSM) Electric Vehicle Based on Simulink. *Energies*, 15(3), 1134.
- Zhao, Y., Zhang, S., Zhang, C., Yang, G., & Yang, Y. (2024). Analysis of cogging torque of permanent magnet motors under mixed-eccentricity and manufacturing tolerances. *IEEE Access*, 12, 6672–6683.

//

Chapter 4

ELECTRICAL ENERGY CONSUMPTION FORECASTING USING ARTIFICIAL INTELLIGENCE

Vekil SARI¹, Volkan GÖREKE²

1 Sivas Cumhuriyet University, Faculty of Engineering, Department of Electrical and Electronics Engineering, 58140, Sivas, Türkiye; e-mail: vsari@cumhuriyet.edu.tr; ORCID: <https://orcid.org/0000-0001-5963-0179>

2 Sivas Cumhuriyet University, Sivas Technical Sciences Vocational School, Department of Computer Technologies, 58140, Sivas, Türkiye; e-mail: vgoreke@cumhuriyet.edu.tr; ORCID: <https://orcid.org/0000-0002-2418-8373>

1. INTRODUCTION

Energy resources can be classified into two categories: primary and secondary energy sources. Primary energy sources consist of non-renewable resources found in nature, such as coal, oil, and natural gas, as well as renewable resources like wind, solar, and hydro energy. Electrical energy, on the other hand, is a secondary energy source produced from primary energy sources (Baltaş and Akbay, 2021).

Electrical energy is one of the most fundamental inputs of modern life. From city lighting to industrial production, from transportation systems to individual households, electricity stands out as an indispensable resource. Since electrical energy cannot be stored, it must be generated in the exact amount required at any given time. Thus, it is essential to predict power demand precisely in order to guarantee the dependability of electricity output. (Zheng et al., 2021).

Accurate prediction of electricity consumption plays a key role in many critical decision-making processes—from energy production to distribution, from cost planning to achieving sustainability goals. Figure 1 shows the classification of energy resources (Koç and Şenel, 2013).

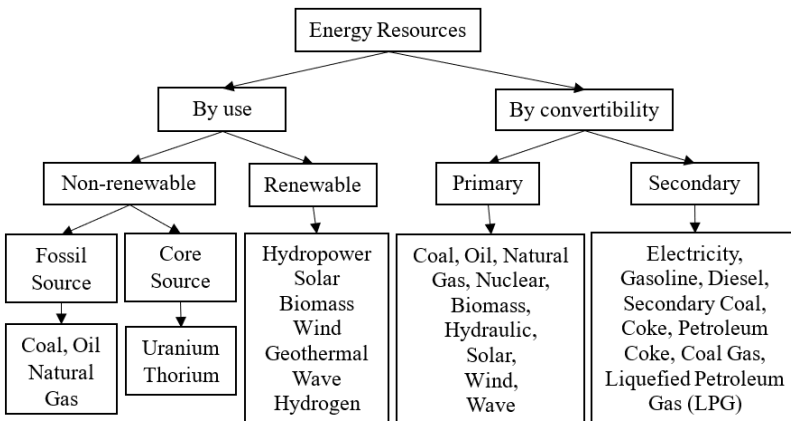


Figure 1. Energy resource classification.

In the electricity market, the task of load forecasting is challenging due to the complex structure of the market. This complexity arises from the instantaneous nature of electricity, the intricate market design, and frequent regulatory interventions (Gökgöz and Filiz, 2020). The demand for electrical energy is driven by meteorological parameters as well as economic and industrial activities. Therefore, accurate region-specific electricity load forecasting can assist in effectively managing, planning,

and scheduling power generation units to reduce unit costs and achieve maximum financial benefit (Jawad et al., 2020).

Forecasts made using traditional methods generally take into account statistical relationships such as trends and seasonality in historical data. However, the variability in consumption habits, the increasing integration of renewable energy sources, and uncertainties in climate conditions have created a need for more flexible and powerful methods. The use of neural networks for electricity energy forecasting has been increasing over time. This rise is due to the ability of neural networks to account for the nonlinear structure of power consumption data and to uncover non-trivial dependencies within them (Klyuev et al., 2022).

Artificial intelligence (AI) can learn multidimensional and complex relationships by simultaneously evaluating past consumption data and external factors (such as weather conditions, calendar information, and economic indicators). In this way, it is possible to make short-, medium-, and long-term consumption forecasts with higher accuracy. Moreover, AI-based methods can provide not only a single forecast value but also uncertainty intervals, offering decision-makers more reliable information.

Based on the forecasting time frame, there are four types of electricity load forecasting: long-term, medium-term, short-term, and very short-term load forecasting. Very short-term forecasting concerns load predictions within time intervals ranging from minutes to an hour. It focuses on near-future forecasts, often considering time and temperature, and explores current values to estimate future ones. Very short-term forecasting primarily depends on the most recent load patterns. Short-term forecasting involves time periods ranging from several minutes to days and represents a key factor in the daily operation and planning of an energy company, being a critical component of an energy management system. The short-term approach is effective in reducing financial costs and operational risks, directly influencing savings; therefore, it holds great importance in a competitive energy market.

Medium-term forecasting generally deals with time intervals ranging from one month to one year and covers activities such as planning grid maintenance, evaluating electricity prices, organizing energy sharing, and planning fuel usage. Long-term forecasting aims to estimate electricity demand over periods longer than a year, including demand planning for various power systems. It helps ensure system understanding, reliable operation of the power supply, and the ability to meet future demands.

For these time horizons, various forecasting methods can be used, in-

cluding knowledge-based expert systems, statistical techniques, machine learning models, AI techniques, hybrid techniques, and deep learning models (Azeem et al., 2021).

Numerous studies have been conducted on forecasting electrical energy consumption. In one such study (Demirel et al., 2010), electricity demand forecasts were made using the Adaptive Network-Based Fuzzy Inference System (ANFIS) and Autoregressive Moving Average (ARMA) techniques. The results showed that the ANFIS model produced significantly better outcomes compared to the ARMA model.

In another study (Akmaz, 2022), a method was developed for forecasting Turkey's electricity consumption. In this method, the Correlation-Based Feature Selection Method, Curve Fitting technique, and Multilayer Perceptron Algorithm were used. The application results showed that the method performed successfully on historical data.

In a study conducted by Özkan et al. (2020), forecasting models for electricity consumption data were developed using the "Fourier Analysis with the Least Squares Method" and the "Winters Method" in time series analysis. By dividing the dataset into 12-, 24-, and 36-month periods, the relationship between the coefficient of variation in each period and the performance of the forecasting models was analyzed.

Ülkü and Yalpır (2021) generated scenarios for forecasting Turkey's provincial electricity demand for the year 2030 using data from 2009–2018 by applying Artificial Neural Networks (ANN) and Multiple Regression Analysis (MRA) methods.

In another study (Oğcu et al., 2012), Support Vector Regression (SVR) and ANN models were used to develop the best model for predicting electricity production in 2010 and 2011. A seasonal SVR model was proposed to forecast seasonal time series data. The study demonstrated that the seasonal SVR model outperformed the ANN model.

In the study by Bişkin and Çifci (2021), deep learning methods such as Long Short-Term Memory (LSTM) and Gated Recurrent Unit (GRU) models were utilized to predict power usage using time series data. Using historical electricity consumption data from Turkey, one-hour and three-hour ahead forecasts were generated. Comparison results indicated that the GRU model performed slightly better than the LSTM model.

Başoğlu and Bulut (2016) developed a hybrid system called EPSİM-NN by combining artificial neural networks and expert systems. Using data from the past ten years, this system was applied for short-term electricity

demand forecasting. The EPSİM-NN system produced predictions close to actual values for short-term periods.

Çayır et al. (2018) developed a short-term consumption forecasting model using machine learning algorithms with three years of electricity power consumption data from 30 households in a district of London, United Kingdom. The results showed that the Random Forest (RF) method was the most suitable model for the daily electricity consumption problem.

In another study (Haliloğlu and Tutu, 2018), daily data from January 2012 to April 2018 were used to construct a model based on the Least Squares Method (LSM). The model included independent variables such as the temperature threshold difference, previous day's electricity consumption, and time dummy variables. This model achieved an electricity demand estimation accuracy of 92.8%.

Kamber et al. (2021) used Spain's electricity data from 2015–2016. In this study, hourly electricity consumption data were analyzed using the LSTM method, and the results were compared with time series analysis outcomes. Both an LSTM model and an ARIMA model were developed, and their forecasting performances were compared.

Turkey's power production and demand were predicted by Şahin (2018). The Gray Forecasting Method was used in this study. According to the findings, the posterior error ratio (C) and small error probability (p) for the GM(1,1) model of Turkey's electricity production were 0.12 and 0.97, respectively, but the corresponding p and C values for electricity consumption were 0.11 and 0.97.

In another study (Pierre et al., 2023), five approaches were examined for forecasting electricity consumption: ARIMA, LSTM, GRU, ARIMA-LSTM, and ARIMA-GRU. The results revealed that the hybrid ARIMA-LSTM approach achieved better accuracy with an RMSE of 7.35. These findings indicate that hybrid approaches perform better than single models in predicting electricity consumption.

Wu and Wu (2024) proposed a new CNN-BiLSTMSA model that combines a Convolutional Neural Network (CNN), Bidirectional Long Short-Term Memory (BiLSTM), and Self-Attention (SA) mechanisms to accurately forecast household electricity consumption. The proposed model integrates temporal feature extraction through the CNN module, correlation capture through BiLSTM, and intrinsic feature analysis through the SA mechanism, thereby improving prediction accuracy. The results demonstrated that the model achieved higher precision and out-

performed existing methods in key performance metrics.

2. CHARACTERISTICS OF ELECTRICAL ENERGY CONSUMPTION DATA

A time series is defined as a sequential data set obtained by measuring one or more variables over a specific period (Nebati et al., 2021). Electricity consumption data, by its nature, has the characteristics of a time series. Therefore, it possesses certain statistical and structural properties. These properties can be categorized into four main groups: seasonality, trend, external effects, and noise.

2.1. Seasonality

Consumption exhibits recurring fluctuations within a day (morning–evening), within a week (weekdays–weekends), and within a year (seasons).

2.2. Trend

In the long term, factors such as economic growth, population increase, or energy efficiency policies create upward or downward tendencies in consumption.

2.3. External Effects

Weather conditions (temperature, humidity, wind), special days (holidays, national celebrations), and extraordinary events (natural disasters, pandemics) have direct impacts on consumption.

2.4. Noise

Unexpected fluctuations may occur in the consumption series due to factors such as measurement errors, meter malfunctions, or data loss.

These characteristics determine the modeling approach to be used. For instance, periodic features can be employed to capture seasonal patterns, while weather and calendar data can be incorporated to account for external effects. The reliability and consistency of the data are crucial for the success of artificial intelligence–based forecasts.

3. DATA PREPARATION AND PREPROCESSING

To achieve accurate forecasts using artificial intelligence methods, data must be properly prepared. The data preparation process plays at least as significant a role in model performance as the choice of algorithm. The dataset is prepared for the operational capabilities of AI models by

a sequence of data pretreatment activities, including data cleaning, data integration, data transformation, and data reduction (Geyikoğlu and Yağanoğlu, 2025).

The process of scaling all input data within a specific range (commonly between 0 and 1) is called normalization. Normalization is applied to raw data to make it suitable for model training. If normalization is not applied to the raw dataset, the training of the ANN (Artificial Neural Network) can become very slow. The normalization method selected directly affects the performance of the ANN, as normalization regularizes the distribution of values in the dataset. Extremely large or small input values may appear in the data, possibly due to errors. These outliers can mislead the network (Uygur, 2019).

For effective training of the network, parameters that influence algorithm speed must be correctly determined. These parameters include the learning rate (LR), momentum (M), number of neurons, and number of hidden layers (Güç, 2016).

High-frequency components in time series can introduce noise effects, complicating the modeling process. To suppress such fluctuations and obtain more stable predictions, the moving average (rolling mean) technique can be used. Additionally, to remove the effect of seasonality in the time series, the Fast Fourier Transform (FFT) can be applied.

3.1. Data Sources

- **Electric Energy Consumption Data:** Can be obtained from smart meters, Supervisory Control and Data Acquisition (SCADA) systems, and billing records.
- **Meteorological Data:** includes meteorological data like temperature, humidity, wind speed, and length of sunshine.
- **Calendar Data:** Consists of information on weekdays/weekends, public holidays, and special days.
- **Economic Data:** Includes indicators such as industrial production, electricity prices, and regional demand trends.

3.2. Data Cleaning and Organization

- **Missing Data:** Missing values can be filled using forward/backward filling, interpolation, or model-based methods.
- **Outliers:** Values caused by measurement errors or unusual events can be detected and corrected.

- **Time Alignment:** Inconsistencies arising from daylight saving time changes or different time zones can be adjusted.

4. ELECTRICITY CONSUMPTION FORECASTING METHODS

Many methods are used to forecast electricity consumption. The quantity of data, the extent of the issue, and the required degree of precision all influence the approach selection. The most commonly used forecasting methods include: Artificial Neural Network (ANN), Support Vector Machine (SVM), Autoregressive Integrated Moving Average (ARIMA), Random Forest (RF), Decision Trees (DT), Long Short-Term Memory (LSTM), Particle Swarm Optimization (PSO), k-Nearest Neighbors (KNN), Fuzzy Logic, Extreme Gradient Boosting (XGBoost), Curve Fitting Algorithm (CFA), Recurrent Neural Network (RNN), Convolutional Neural Network (CNN), Quantile Regression (QR), and Autoregressive Distributed Lag (ARDL) (Nti et al., 2020).

By combining different methods, hybrid systems can be created. These systems (e.g., ARIMA + XGBoost) integrate the strengths of each method to produce more accurate results (Pierre et al., 2023; Wu and Wu, 2024; Yanan et al., 2023).

Electric energy consumption forecasting methods can generally be grouped into three main categories: Traditional Forecasting Techniques, Modified Traditional Techniques, and Computer Software-Based Techniques (Unutmaz, 2022).

4.1. Traditional Forecasting Methods

These methods enable forecasting using mathematical techniques. Traditional forecasting methods include regression analysis, exponential smoothing, and iteratively reweighted least squares.

4.1.1. Regression Analysis

Regression analysis can be defined as determining an unknown situation based on known values. This method involves dependent and independent variables. When creating the model, the independent variable can be one or more, depending on the desired outcome. Regression not only explains the relationship between variables but also allows predicting unknown situations from known data (Kaysal et al., 2022).

4.1.2. Least Squares Method

By minimizing the squares of the errors between actual and anticipated values, the least squares approach is a modeling technique that estab-

lishes a function between variables (Biçer, 2018).

4.2. Modified Traditional Techniques

To improve forecasting models under changing load conditions, adaptive demand forecasting and probabilistic time series techniques are used.

4.2.1. Time Series Analysis

In time series analysis, historical data are examined to determine whether a specific trend exists, and future predictions are made accordingly. A sequence of values representing changes over time in past data constitutes a time series. Time series analysis investigates the patterns of these changes and develops a model that represents the behavior of the process. This model is then used to forecast future demand (Yazıcıoğlu, 2010).

Time series analyses include four Box-Jenkins models: Autoregressive (AR), Moving Average (MA), Autoregressive Moving Average (ARMA), and Autoregressive Integrated Moving Average (ARIMA). The ARIMA method is a widely used statistical time series model in statistics and econometrics (Boltürk, 2013). ARIMA is a classical statistical model that forecasts the future based on historical data and does not use “learning” or network structures like artificial intelligence or machine learning models.

4.3. Computer Software-Based Techniques

These techniques have become widely used in recent years by providing an effective and efficient approach in systems where precise modeling is difficult or uncertain. Computer software-based techniques include genetic algorithms, fuzzy logic, and artificial neural networks (ANNs).

The concepts of artificial intelligence (AI), machine learning (ML), and deep learning (DL) are often confused. Generally, AI refers to systems and machines that perform specific tasks, which may require human involvement and/or intelligence. Machine learning consists of algorithms that learn from data and analyze data patterns. Based on these patterns, ML can make decisions. Compared to AI, this process requires less human involvement, but humans can still intervene if a decision is incorrect. Deep learning, on the other hand, does not require human intervention and achieves accurate results using neural networks. The connection between AI, ML, and DL is illustrated in Figure 2 (Köse, 2023).

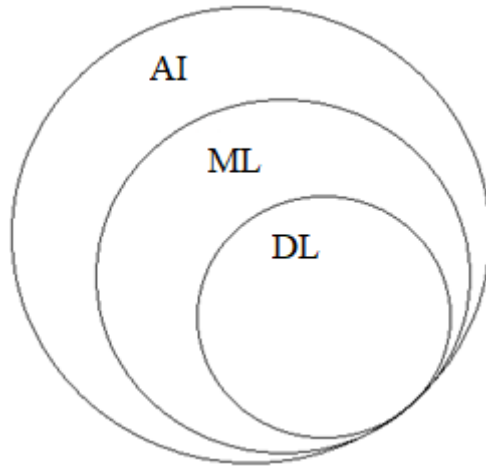


Figure 2. *The connection between AI, ML, and DL.*

4.3.1. Artificial Neural Networks (ANNs)

Many techniques for predicting the demand for electricity have been developed in recent years. Statistical models, parametric methods, and learning-based forecasting approaches have been adopted. Among these, methods based on artificial intelligence algorithms have gained prominence, particularly because they provide very good forecasting results for nonlinear and complex problems (Akman et al., 2018).

Artificial Neural Networks (ANNs) were inspired by the functioning of the human brain and were first proposed in 1943. The aim of ANNs is to mathematically model human brain cells and emulate them within a computer system. In humans, learning occurs through the connections between synapses. Depending on the network type, ANNs are generally categorized as feedforward, multilayer, or feedback (recurrent) networks. Figure 3 illustrates a model of a single neuron (Sarı and Göreke, 2024).

From a learning strategy perspective, ANNs are generally divided into three categories: supervised learning, unsupervised learning, and reinforcement learning (Pençe et al., 2019).

- **Supervised Learning:** This refers to a system that has an output variable (dependent variable) and one or more input variables (independent variables). The algorithm trains the model to map inputs to outputs.
- **Unsupervised Learning:** In this type, only input variables exist in the dataset, with no output variable. The machine derives mean-

ingful patterns from the existing data. By grouping the input variables, the machine uncovers inherent structures or distributions. In order to learn more about the data, unsupervised learning aims to model its underlying structure or distribution.

- **Reinforcement Learning:** This is inspired by behavioral science. For example, a crawling baby repeatedly falls while learning to walk, gradually learning from each fall until it can walk. In reinforcement learning, an agent tries to perform a task constrained by the environment. After each action, the agent receives a reward. The goal is for the agent to learn to perform the task optimally based on the rewards received (Şen, 2022).

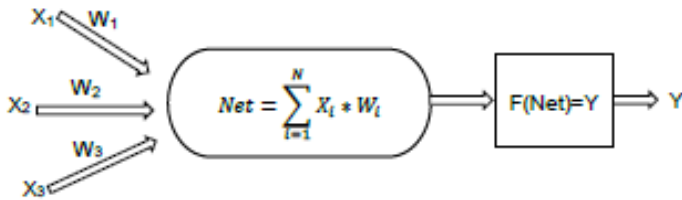


Figure 3. Neuron Model.

4.3.2. Model Validation

The data are divided into two parts: training and testing. The model is trained using a portion of the data, and its performance is tested using a separate fraction. This way, the accuracy of the model can be assessed using data that were not involved in training. Testing should not be performed using the data used for training.

Model validation is particularly important when the available data are limited. One technique for evaluating models that shows how well a learner can predict on unknown data is cross-validation. If the entire dataset is used solely for training, the learner may memorize the data and produce perfect predictions for the same values but will have no information on how it will perform with unseen data. This problem is known as overfitting. To overcome this, a portion of the dataset should be reserved as test data that the learner has never seen during training (Pençe et al., 2019). In time series forecasting, special validation methods that use future data are preferred.

4.3.3. Performance Metrics

No forecasting method provides perfectly accurate results. Every method has a certain level of error in its predictions. The statistical metrics used to measure the accuracy of a forecasting model are called performance metrics. The most commonly used metrics include Mean Absolute Error (MAE), Mean Squared Error (MSE), Root Mean Square Error (RMSE), Mean Absolute Percentage Error (MAPE), and the R^2 coefficient (Jawad et al., 2020; Demirel et al., 2010; Özkan et al., 2020; Wu and Wu, 2024; Yanan et al., 2023).

- **Mean Absolute Error (MAE):** The average of the absolute differences between predicted and actual values. Since absolute values are used, MAE is always positive. A smaller MAE indicates a more accurate model.

$$MAE = \frac{1}{N} \sum_{i=1}^N |z_i - y_i| \quad (1)$$

- **Mean Squared Error (MSE):** The average of the squares of the differences between actual and predicted values. Squaring ensures a positive value. A smaller MSE indicates predictions closer to actual values.

$$MSE = \frac{1}{N} \sum_{i=1}^N (z_i - y_i)^2 \quad (2)$$

- **Root Mean Square Error (RMSE):** The square root of the average of the squared differences between predicted and actual values. RMSE is always positive and is sensitive to large errors.

$$RMSE = \sqrt{\frac{1}{N} \sum_{i=1}^N (z_i - y_i)^2} \quad (3)$$

- **Mean Absolute Percentage Error (MAPE):** Indicates the percentage of prediction errors relative to the actual values.

$$MAPE = \frac{1}{N} \sum_{i=1}^N \left| \frac{z_i - y_i}{z_i} \right| \times 100\% \quad (4)$$

- **R^2 Coefficient:** One of the fundamental statistical measures used to assess model performance. It shows how much of the variance in the dependent variable (the variable to be predicted) is explained by the model. It ranges between 0 and 1, with values closer to 1 indicating a more explanatory model.

$$R^2 = 1 - \frac{\sum_{i=1}^N (z_i - y_i)^2}{\sum_{i=1}^N (y_i - \bar{y}_i)^2} \quad (5)$$

Here, the actual electricity consumption is denoted by z_i , the predicted electricity consumption by y_i , the number of data points in the electricity dataset by N , and the average of the predicted values is denoted by \bar{y}_i .

5. CONCLUSION

Electricity consumption forecasting is becoming increasingly powerful and reliable with the development of artificial intelligence techniques. In the near future, it is expected that high-frequency data obtained from smart meters will enable more detailed and precise forecasts. By processing real-time consumption data, dynamic decision support systems for grid management are anticipated to be developed.

Electricity consumption forecasting models will become even more important for integrating variable generation sources, such as solar and wind, into the grid. The use of cloud-based solutions will increase data storage and computational capacity, enabling applications on a larger scale. In critical sectors like energy, it is expected that forecasting models will not only need to be accurate but also interpretable.

In conclusion, AI-based electricity consumption forecasts will be one of the most important tools shaping the future of the energy sector. When supported by proper data management, appropriate model selection, and reliable evaluation methods, these approaches will contribute to a sustainable, secure, and economical energy future—not only for energy companies but for society as a whole.

Electricity load forecasting can be used by distribution companies for load balancing and preventing outages. Accurate demand forecasts allow for the development of pricing and trading strategies. Flexible forecasts can facilitate the integration of variable energy sources, such as solar and wind, into the system. Consumer energy usage patterns can also be optimized. Forecasting models are not an end in themselves; they form the foundation of decision support mechanisms for energy companies, regulators, and policymakers.

REFERENCES

- Akman, T., Yılmaz, C., & Sönmez, Y. (2018). Elektrik Yükü Tahmin Yöntemlerinin Analizi. *Gazi Journal of Engineering Sciences*, 4(3), 168-175.
- Akmaz, D. (2022). Çok Katmanlı Algılayıcı Algoritması, Korelasyon Tabanlı Özellik Seçme Yöntemi ve Eğri Uydurma Tekniği ile Türkiye’de Toplam Elektrik Tüketiminin Tahmin Edilmesi. *Fırat Üniversitesi Mühendislik Bilimleri Dergisi*, 34(2), 677-686.
- Azeem, A., Ismail, I., Jameel, S. M., & Harindran, V. R. (2021). Electrical Load Forecasting Models for Different Generation Modalities: A Review. *IEEE Access*, 9, 142239-142263.
- Baltaş, M. E., & Akbay, C. (2021). Akdeniz Elektrik Dağıtım Bölgesi (Antalya-Isparta-Burdur) Elektrik Tüketim Talep Tahmini. *Journal of Management and Economics Research*, 19(2), 222-238.
- Başoğlu, B., & Bulut, M. (2017). Kısa Dönem Elektrik Talep Tahminleri için Yapay Sinir Ağları ve Uzman Sistemler Tabanlı Hibrit Sistem Geliştirilmesi. *Journal of the Faculty of Engineering and Architecture of Gazi University*, 32(2), 575-583.
- Biçer, A. (2018). Enerji Talep Tahminine Yönelik Program Geliştirme ve Bir Bölge İçin Uygulaması, *Afyon Kocatepe Üniversitesi, Fen Bilimleri Enstitüsü, Yüksek Lisans Tezi*.
- Bişkin, O. T., & Çifçi, A. (2021). Forecasting of Turkey’s Electrical Energy Consumption using LSTM and GRU Networks. *Bilecik Şeyh Edebali Üniversitesi Fen Bilimleri Dergisi*, 8(2), 656-667.
- Boltürk, E. (2013). Elektrik Talebi Tahmininde Kullanılan Yöntemlerin Karşılaştırılması, *İstanbul Teknik Üniversitesi, Fen Bilimleri Enstitüsü, Yüksek Lisans Tezi*.
- Çayır, A., Yenidoğan, I., & Dağ, H. (2018). Konutların Günlük Elektrik Güç Tüketimi Tahmini için Uygun Model Seçimi. *Fırat Üniversitesi Mühendislik Bilimleri Dergisi*, 30(3), 15-21.
- Demirel, Ö., Kakilli, A., & Tektaş, M. (2010). Anfis ve Arma Modelleri ile Elektrik Enerjisi Yük Tahmini. *Gazi Üniversitesi Mühendislik Mimarlık Fakültesi Dergisi*, 25(3), 601-610.
- Geyikoğlu, A., & Yağanoğlu, M. (2025). Makine Öğrenmesi Algoritmaları ile Elektrik Dağıtım Şebekeleri Arıza Tahmini. *Karadeniz Fen Bilimleri Dergisi*, 15(1), 73-98.
- Gökgöz, F., & Filiz, F. (2020). Electricity Load Forecasting via ANN Approach in Turkish Electricity Markets. *Bilgi Yönetimi Dergisi*, 3(2), 170-184.
- Güç, R. (2016). Bilecik ili için güneş enerjisi analizi ve yapay sinir ağları ile hava sıcaklığı tahmini. *Bilecik Şeyh Edebali Üniversitesi, Fen Bilimleri Enstitüsü, Yüksek Lisans Tezi*.
- Haliloğlu, E. Y., & Tutu, B. E. (2018). Türkiye için Kısa Vadeli Elektrik Enerjisi Talep Tahmini. *Journal of Yasar University*, 13(51), 243-255.
- Jawad, M., Nadeem, M. S. A., Shim, S. O., Khan, I. R., Shaheen, A., Habib, N.,

- Hussain, L., & Aziz, W. (2020). Machine Learning Based Cost Effective Electricity Load Forecasting Model Using Correlated Meteorological Parameters. *IEEE Access*, 8, 146847-146864.
- Kamber, E., Körpüz, S., Can, M., Aydoğmuş, H. Y., & Gümüş, M. (2021). Yapay Sinir Ağlarına Dayalı Kısa Dönemli Elektrik Yüğü Tahmini. *Endüstri Mühendisliği*, 32(2), 364-379.
- Kaysal, K., Akarşlan, E., & Hocaođlu, F. O. (2022). Türkiye Kısa Dönem Elektrik Yüğü Talep Tahmininde Makine Öğrenmesi Yöntemlerinin Karşılaştırılması. *Bilecik Şeyh Edebali Üniversitesi Fen Bilimleri Dergisi*, 9(2), 693-702.
- Klyuev, R. V., Morgoev, I. D., Morgoeva, A. D., Gavrina, O. A., Martuyushev, N. V., Efrementkov, E. A., & Mengxu, Q. (2022). Methods of Forecasting Electric Energy Consumption: A Literature Review. *Energies*, 15, 8919.
- Koç, E., & Şenel, M. C. (2013). Dünyada ve Türkiye’de enerji durumu-genel değerlendirme. *Mühendis ve Makina*, 54(639), 32-44.
- Köse, R. E. (2023). Developing A Decision-Support System Using Machine Learning And Deep Learning Models For Daily Demand Forecasting: A Case Study, İstanbul Teknik Üniversitesi, Lisansüstü Eğitim Enstitüsü, Yüksek Lisans Tezi.
- Nebati, E. E., Taş, M., & Ertaş, G. (2021). Türkiye’de Elektrik Tüketiminde Talep Tahmini: Zaman Serisi ve Regresyon Analizi ile Karşılaştırma. *Avrupa Bilim ve Teknoloji Dergisi*, 31 (Ek Sayı 1), 348-357.
- Nti, I. K., Teimeh, M., Nyarko-Boateng, O., & Adekoya, A. F. (2020). Electricity Load Forecasting: A Systematic Review. *Journal of Electrical Systems and Information Technology*, 7(13), 1-19.
- Oğcu, G., Demirel, O. F., & Zaim, S. (2012). Forecasting Electricity Consumption with Neural Networks and Support Vector Regression. *Procedia-Social and Behavioral Sciences*, 58, 1576-1585.
- Özkan, E., Güler, E., & Aladağ, Z. (2020). Elektrik Enerjisi Tüketim Verileri İçin Uygun Tahmin Yöntemi Seçimi. *Endüstri Mühendisliği*, 31(2), 198-214.
- Pençe, İ., Kalkan, A., & Çeşmeli, M. Ş. (2019). Türkiye Sanayi Elektrik Enerjisi Tüketiminin 2017-2023 Dönemi için Yapay Sinir Ağları ile Tahmini. *Mehmet Akif Ersoy Üniversitesi Uygulamalı Bilimler Dergisi*, 3(2), 206-228.
- Pierre, A. A., Akim, S. A., Semenyoy, A. K., & Babiga, B. (2023). Peak Electrical Energy Consumption Prediction by ARIMA, LSTM, GRU, ARIMA-LSTM, and ARIMA-GRU Approaches. *Energies*, 16, 4739.
- Sarı, V., & Göreke, V. (2024). Elektrik Motorlarının Arızalarının Tespitinde Yapay Zeka Yöntemlerinin Kullanılması. *Yapay Zeka ve Makine Öğrenimi ile Mühendislikte Yenilikçi Yaklaşımlar*, 105.
- Şahin, U. (2018). Forecasting of Turkey’s Electricity Generation and Consumption with Grey Prediction Method. *Mugla Journal of Science and Technology*, 4(2), 205-209.
- Şen, E. (2022). Elektrikli Araçların Enerji Talep Tahmini, Erciyes Üniversitesi,

Fen Bilimleri Enstitüsü, Yüksek Lisans Tezi.

- Unutmaz, Y. E. (2022). Dağıtık Üretim Sistemleri İçin Optimizasyon Yöntemlerinin İncelenmesi ve Yapay Sinir Ağları ile Talep Tahmini, Yıldız Teknik Üniversitesi, Fen Bilimleri Enstitüsü, Yüksek Lisans Tezi.
- Uygur, S. (2019). Bir Gıda İşletmesinde Enerji Talep Tahmini, Bursa Uludağ Üniversitesi, Fen Bilimleri Enstitüsü, Yüksek Lisans Tezi.
- Ülkü, H., & Yalçır, Ş. (2021). Enerji Talep Tahmini İçin Metodoloji Geliştirme: 2030 Yılı Türkiye Örneği. Niğde Ömer Halisdemir Üniversitesi Mühendislik Bilimleri Dergisi, 10(1), 188-201.
- Wu, M. P., & Wu, F. (2024). Predicting Residential Electricity Consumption Using CNN-BILSTM-SA Neural Networks. IEEE Access, 12, 71555-71565.
- Yanan, W., Jiekang, W., & Zhen, L. (2023). A Hybrid Model for Short-Term Load Forecasting Based on Novel Input Sequence Selection and CSO Optimized Depth Belief Network. IEEE Access, 11, 116141-116152.
- Yazıcıoğlu, N. (2010). Yapay Zeka İle Talep Tahmini. Uludağ Üniversitesi, Fen Bilimleri Enstitüsü, Yüksek Lisans Tezi.
- Zheng, K., Li, P., Zhou, S., Zhang, W., Li, S., Zeng, L., & Zhang, Y. (2021). A Multi-Scale Electricity Consumption Prediction Algorithm Based on Time-Frequency Variational Autoencoder. IEEE Access, 9, 90937-90946.